SLAC–PUB–9056
November 2001

QCD Phenomenology and Light-Front Wavefunctions *

Stanley J. Brodsky
Stanford Linear Accelerator Center
Stanford University, Stanford, California 94309
sjbth@slac.stanford.edu

Invited lectures, presented at the
Cracow School Of Theoretical Physics:
41st Course: Fundamental Interactions
Zakopane, Poland
2–11 June 2001

*Work supported by the Department of Energy under contract number DE-AC03-76SF00515.

Abstract

A natural calculus for describing the bound-state structure of relativistic composite systems in quantum field theory is the light-front Fock expansion which encodes the properties of a hadrons in terms of a set of frame-independent $n-$particle wavefunctions. Light-front quantization in the doubly-transverse light-cone gauge has a number of remarkable advantages, including explicit unitarity, a physical Fock expansion, the absence of ghost degrees of freedom, and the decoupling properties needed to prove factorization theorems in high momentum transfer inclusive and exclusive reactions. A number of applications are discussed in these lectures, including semileptonic B decays, two-photon exclusive reactions, diffractive dissociation into jets, and deeply virtual Compton scattering. The relation of the intrinsic sea to the light-front wavefunctions is discussed. Light-front quantization can also be used in the Hamiltonian form to construct an event generator for high energy physics reactions at the amplitude level. The light-cone partition function, summed over exponentially-weighted light-cone energies, has simple boost properties which may be useful for studies in heavy ion collisions. I also review recent work which shows that the structure functions measured in deep inelastic lepton scattering are affected by final-state rescattering, thus modifying their connection to light-front probability distributions. In particular, the shadowing of nuclear structure functions is due to destructive interference effects from leading-twist diffraction of the virtual photon, physics not included in the nuclear light-cone wavefunctions.

1 Introduction

Progress in the development and testing of quantum chromodynamics will require a detailed understanding of hadron processes at the amplitude level. For example, exclusive B-meson decays depend critically on the wavefunction of the B as well as the final-state hadronic wavefunctions. Spin correlations such as single-spin asymmetries in hard QCD reactions, require an understanding of the phase structure of hadron amplitudes, physics well beyond that contained in probability distributions.

One of the challenges of relativistic quantum field theory is to compute the wavefunctions of bound states, such as the amplitudes which determine the quark and gluon substructure of hadrons in quantum chromodynamics. However, any extension of the Heisenberg-Schrödinger formulation of quantum mechanics $H|\,\psi\rangle = i\frac{\partial}{\partial t}|\,\psi\rangle = E|\,\psi\rangle$ to the relativistic domain has to confront seemingly intractable hurdles: (1) quantum fluctuations preclude finite particle-number wavefunction representations; (2) the charged particles arising from the quantum fluctuations of the vacuum contribute to the matrix element of currents – thus knowledge of the wavefunctions alone is insufficient to determine observables; and (3) the boost of an equal-time wavefunction from one Lorentz frame to another not only changes particle number, but is as complicated a dynamical problem as solving for the wavefunction itself.

In 1949, Dirac [1] made the remarkable observation that ordinary "instant" time t is not the only possible evolution parameter. In fact, evolution in "light-front" time $\tau = t + z/c = x^+$ has extraordinary advantages for relativistic systems, stemming from the fact that 7 out of the 10 Poincare' generators, including a Lorentz boost K_3, are kinematical (interaction-independent) when one quantizes a theory at fixed light-front time.

The light-front fixes the initial boundary conditions of a composite system as its constituents are intercepted by a light-wave evaluated on the hyperplane $x^+ = t+z/c$. In contrast, determining an atomic wavefunction at a given instant $t = t_0$ requires measuring the simultaneous scattering of Z photons on the Z electrons. In fact, the Fock-state representation of bound states defined at equal light-cone time, *i.e.*, along the light-front, provides wavefunctions of fixed particle number which are independent of the eigenstate's four-momentum P^μ. Furthermore, quantum fluctuations of the vacuum are absent if one uses light-front time to quantize the system, so that matrix elements such as the electromagnetic form factors only depend on the currents of the constituents described by the light-cone wavefunctions. I will use here the notation $A^\mu = (A^+, A-, A_\perp)$, where $A^\pm = A^0 \pm A^z$, and the metric is $A \cdot B = \frac{1}{2}(A^+B^- + A^-B^+) - A_\perp \cdot B_\perp$.

In Dirac's "Front Form", the generator of light-front time translations is $P^- = i\frac{\partial}{\partial\tau}$. Boundary conditions are set on the transverse plane labelled by $x_\perp$ and $x^- = z - ct$. See Fig. 1. Given the Lagrangian of a quantum field theory, P^- can be constructed as an operator on the Fock basis, the eigenstates of the free theory. Since each particle in the Fock basis is on its mass shell, $k^- \equiv k^0 - k^3 = \frac{k_\perp^2+m^2}{k^+}$, and its energy $k^0 = \frac{1}{2}(k^+ + k^-)$ is positive, only particles with positive momenta $k^+ \equiv k^0 + k^3 \geq 0$ can occur in the Fock basis. Since the total plus momentum $P^+ = \sum_n k_n^+$ is conserved, the light-cone vacuum cannot have any particle content. The operator $H_{LC} = P^+P^- - P_\perp^2$, the "light-cone Hamiltonian", is frame-independent.

The Heisenberg equation on the light-front is

$$H_{LC}|\,\Psi\rangle = M^2|\,\Psi\rangle \ . \tag{1}$$

This can in principle be solved by diagonalizing the matrix $\langle n|H_{LC}|m\rangle$ on the free Fock basis: [2]

$$\sum_m \langle n|H_{LC}|m\rangle \langle m|\psi\rangle = M^2 \langle n|\Psi\rangle \ . \tag{2}$$

For example the interaction terms of QCD are illustrated in Fig. 2. The eigenvalues $\{M^2\}$ of $H_{LC} = H^0_{LC} + V_{LC}$ give the squared invariant masses of the bound and continuum spectrum of the theory. The light-front Fock space is the eigenstates of the free light-front Hamiltonian; *i.e.*, it is a Hilbert space of non-interacting quarks

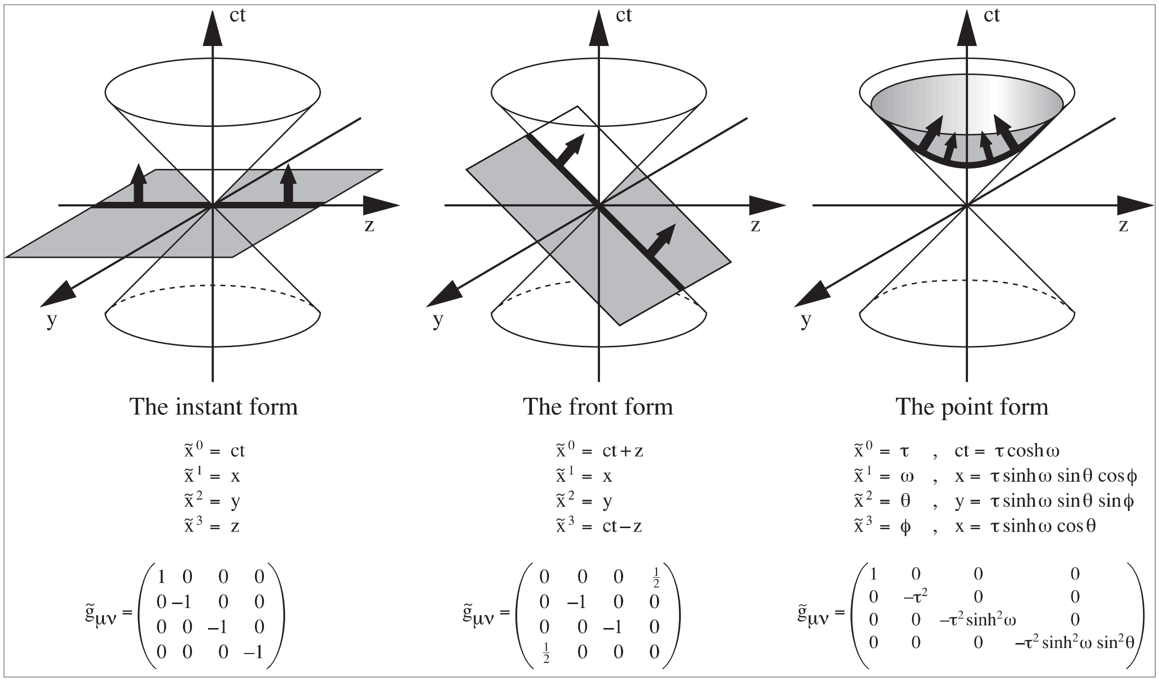

Figure 1: Dirac's three forms of Hamiltonian dynamics. From Ref. [2].

and gluons, each of which satisfy $k^2 = m^2$ and $k^- = \frac{m^2+k^2_\perp}{k^+} \geq 0$. The projections $\{\langle n|\Psi\rangle\}$ of the eigensolution on the n-particle Fock states provide the light-front wavefunctions. Thus solving a quantum field theory is equivalent to solving a coupled many-body quantum mechanical problem:

$$[M^2 - \sum_{i=1}^{n} \frac{m^2_{\perp i}}{x_i}]\psi_n = \sum_{n'} \int \langle n|V_{LC}|n'\rangle\, \psi_{n'} \tag{3}$$

where the convolution and sum is understood over the Fock number, transverse momenta, plus momenta, and helicity of the intermediate states. Here $m^2_\perp = m^2 + k^2_\perp$. An essentially equivalent approach to light-front quantization, pioneered by Weinberg [3, 4], is to evaluate the equal-time theory from the perspective of an observer moving in the negative $\hat{z}$ direction with arbitrarily large momentum $P_z \to -\infty$. The light-cone fraction $x = \frac{k^+}{p^+}$ of a constituent can be identified with the longitudinal momentum $x = \frac{k^z}{P^z}$ in a hadron moving with large momentum P^z. Light-front wavefunctions are also related to momentum-space Bethe-Salpeter wavefunctions by integrating over the relative momenta $k^- = k^0 - k^z$ since this projects out the dynamics at $x^+ = 0$.

We can compare the light-front Fock expansion with the n-particle Schrödinger momentum space wavefunction $\psi_N(\vec{p}_i)$ of a composite system is the projection of the exact eigenstate of the equal-time Hamiltonian on the n-particle states of the non-interacting Hamiltonian, the Fock basis. It represents the amplitude for

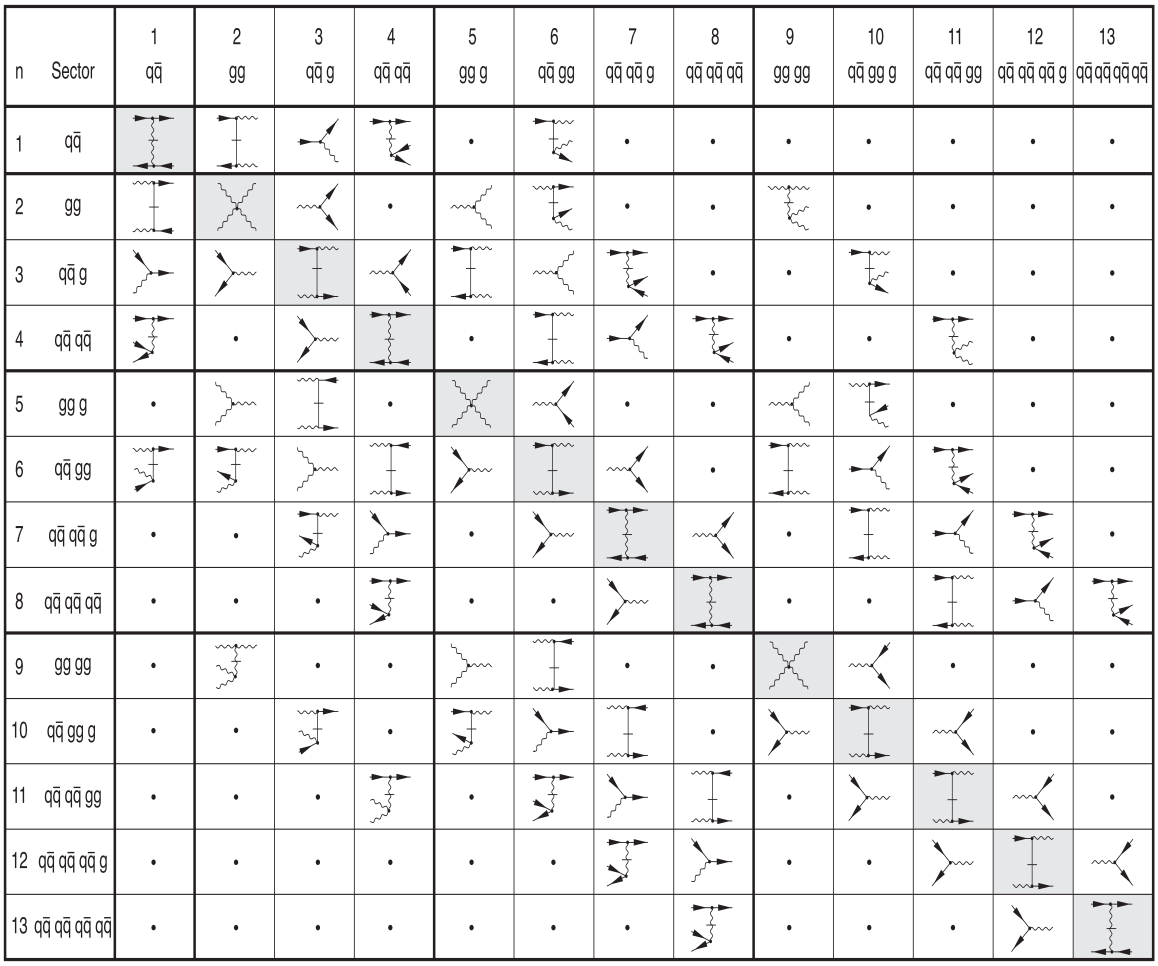

Figure 2: The front-form matrix of QCD interactions in light-cone gauge. Up to eight constituents in a meson are shown. From Ref. [2] and H. C. Pauli.

finding the constituents with three-momentum $\vec{p}_i$, orbital angular momentum, and spin, subject to three-momentum conservation and angular momentum sum rules. The constituents are on their mass shell, $E_i = \sqrt{\vec{p}_i^2 + m_i^2}$ but do not conserve energy $\sum_{i=1}^n E_i > E = \sqrt{\vec{p}^2 + M^2}$. However, in a relativistic quantum theory, a bound-state cannot be represented as a state with a fixed number of constituents. For example, the existence of gluons which propagate between the valence quarks necessarily implies that the hadron wavefunction must describe states with an arbitrary number of gluons. Thus a hadronic wavefunction must describe fluctuations in particle number n, as well as momenta and spin. One has to take into account fluctuations in the wavefunction which allow for any number of sea quarks, as long as the total quantum numbers of the constituents are compatible with the overall quantum numbers of the baryon.

It is especially convenient to develop the light-front formalism in the light-cone gauge $A^+ = A^0 + A^z = 0$. In this gauge the A^- field becomes a dependent degree of freedom, and it can be eliminated from the gauge theory Hamiltonian, with the addition of a set of specific instantaneous light-front time interactions. In fact in $QCD(1+1)$ theory, this instantaneous interaction provides the confining linear x^- interaction between quarks. In $3+1$ dimensions, the transverse field $A^\perp$ propagates massless spin-one gluon quanta with polarization vectors [5] which satisfy both the gauge condition $\epsilon_\lambda^+ = 0$ and the Lorentz condition $k \cdot \epsilon = 0$. Thus no extra condition on the Hilbert space is required.

In QCD, the wavefunction of a hadron describes its composition in terms of the momenta and spin projections of quark and gluon constituents. For example, the eigensolution of a negatively-charged meson QCD, projected on its color-singlet $B = 0$, $Q = -1$, $J_z = 0$ eigenstates $\{|\, n\rangle\}$ of the free Hamiltonian $H_{LC}^{QCD}(g=0)$ at fixed $\tau = t - z/c$ has the expansion:

$$\begin{aligned}\left|\Psi_M; P^+, \vec{P}_\perp, \lambda\right\rangle &= \sum_{n\geq 2,\lambda_i} \int \Pi_{i=1}^n \frac{d^2 k_{\perp i} dx_i}{\sqrt{x_i} 16\pi^3} 16\pi^3 \delta\left(1 - \sum_j^n x_j\right) \delta^{(2)}\left(\sum_\ell^n \vec{k}_{\perp \ell}\right) \\ &\quad \left|n; x_i P^+, x_i \vec{P}_\perp + \vec{k}_{\perp i}, \lambda_i\right\rangle \psi_{n/M}(x_i, \vec{k}_{\perp i}, \lambda_i). \qquad (4)\end{aligned}$$

The set of light-front Fock state wavefunctions $\{\psi_{n/M}\}$ represent the ensemble of quark and gluon states possible when the meson is intercepted at the light-front. The light-front momentum fractions $x_i = k_i^+/P_\pi^+ = (k^0 + k_i^z)/(P^0 + P^z)$ with $\sum_{i=1}^n x_i = 1$ and $\vec{k}_{\perp i}$ with $\sum_{i=1}^n \vec{k}_{\perp i} = \vec{0}_\perp$ represent the relative momentum coordinates of the QCD constituents and are independent of the total momentum of the state.

Remarkably, the light-front wavefunctions $\psi_{n/p}(x_i, \vec{k}_{\perp i}, \lambda_i)$ are independent of the proton's momentum $P^+ = P^0 + P^z$, and $P_\perp$. Thus once one has solved for the light-front wavefunctions, one can compute hadron matrix elements of currents between hadronic states of arbitrary momentum. The actual physical transverse momenta are $\vec{p}_{\perp i} = x_i \vec{P}_\perp + \vec{k}_{\perp i}$. The λ_i label the light-front spin S^z projections of the quarks and gluons along the quantization z direction. The spinors of the light-front formalism automatically incorporate the Melosh-Wigner rotation. The physical gluon polarization vectors $\epsilon^\mu(k,\ \lambda = \pm 1)$ are specified in light-cone gauge by the conditions $k \cdot \epsilon = 0,\ \eta \cdot \epsilon = \epsilon^+ = 0$. The parton degrees of freedom are thus all physical; there are no ghost or negative metric states.

The light-front representation thus provides a frame-independent, quantum-mechanical representation of a hadron at the amplitude level, capable of encoding its multi-quark, hidden-color and gluon momentum, helicity, and flavor correlations in the form of universal process-independent hadron wavefunctions.

Angular momentum has simplifying features in the light-front formalism since the projection J_z is kinematical and conserved. Each light-front Fock wavefunction satisfies the angular momentum sum rule: $J^z = \sum_{i=1}^n S_i^z + \sum_{j=1}^{n-1} l_j^z$. The sum over S_i^z represents the contribution of the intrinsic spins of the n Fock state constituents. The sum over orbital angular momenta

$$l_j^z = -\mathrm{i}\left(k_j^1 \frac{\partial}{\partial k_j^2} - k_j^2 \frac{\partial}{\partial k_j^1}\right) \tag{5}$$

derives from the $n-1$ relative momenta. This excludes the contribution to the orbital angular momentum due to the motion of the center of mass, which is not an intrinsic property of the hadron. The numerator structure of the light-front wavefunctions is in large part determined by the angular momentum constraints.

If one imposes periodic boundary conditions in $x^- = t + z/c$, then the plus momenta become discrete: $k_i^+ = \frac{2\pi}{L} n_i, P^+ = \frac{2\pi}{L} K$, where $\sum_i n_i = K$ [6, 7]. For a given "harmonic resolution" K, there are only a finite number of ways positive integers n_i can sum to a positive integer K. Thus at a given K, the dimension of the resulting light-front Fock state representation of the bound state is rendered finite without violating Lorentz invariance. The eigensolutions of a quantum field theory, both the bound states and continuum solutions, can then be found by numerically diagonalizing a frame-independent light-front Hamiltonian H_{LC} on a finite and discrete momentum-space Fock basis. Solving a quantum field theory at fixed light-front time τ thus can be formulated as a relativistic extension of Heisenberg's matrix mechanics. The continuum limit is reached for $K \to \infty$. This formulation of the non-perturbative light-front quantization problem is called "discretized light-cone quantization" (DLCQ) [7]. Lattice gauge theory has also been used to calculate the pion light-front wavefunction [8].

The DLCQ method has been used extensively for solving one-space and one-time theories [2], including applications to supersymmetric quantum field theories [9] and specific tests of the Maldacena conjecture [10]. There has been progress in systematically developing the computation and renormalization methods needed to make DLCQ viable for QCD in physical spacetime. For example, John Hiller, Gary Mc-

Cartor, and I [11] have shown how DLCQ can be used to solve 3+1 theories despite the large numbers of degrees of freedom needed to enumerate the Fock basis. A key feature of our work is the introduction of Pauli Villars fields to regulate the UV divergences and perform renormalization while preserving the frame-independence of the theory. A recent application of DLCQ to a 3+1 quantum field theory with Yukawa interactions is given in Ref. [11]. There has also been important progress using the transverse lattice, essentially a combination of DLCQ in 1+1 dimensions together with a lattice in the transverse dimensions [12, 13, 14]. One can also define a truncated theory by eliminating the higher Fock states in favor of an effective potential [15]. Spontaneous symmetry breaking and other nonperturbative effects associated with the instant-time vacuum are hidden in dynamical or constrained zero modes on the light-front. An introduction is given in Refs. [16, 17].

Because of their Lorentz invariance, it is particularily easy to write down exact expressions for matrix elements of currents and other local operators, even the couplings of gravitons. In fact as I discuss in Section 3, one can show that the anomalous gravito-magnetic moment $B(0)$, analogous to $F_2(0)$ in electromagnetic current interactions, vanishes identically for any system, composite or elementary [18]. This important feature which follows in general from the equivalence principle, is obeyed explicitly in the light-front formalism.

The set of light-front wavefunctions provide a frame-independent, quantum-mechanical description of hadrons at the amplitude level capable of encoding multi-quark and gluon momentum, helicity, and flavor correlations in the form of universal process-independent hadron wavefunctions. Matrix elements of spacelike currents such as the spacelike electromagnetic form factors have an exact representation in terms of simple overlaps of the light-front wavefunctions in momentum space with the same x_i and unchanged parton number [19, 20, 21]. The measurement and interpretation of the basic parameters of the electroweak theory and CP violation depends on an understanding of the dynamics and phase structure of B decays at the amplitude level. The light-front Fock representation is specially advantageous in the study of exclusive B decays. For example, we can write down an exact frame-independent representation of decay matrix elements such as $B \to D\ell\overline{\nu}$ from the overlap of $n' = n$ parton conserving wavefunctions and the overlap of $n' = n - 2$ from the annihilation of a quark-antiquark pair in the initial wavefunction [22]. The handbag contribution to the leading-twist off-forward parton distributions measured in deeply virtual Compton scattering have a similar light-front wavefunction representation as overlap integrals of light-front wavefunctions [23, 24]. I will review this application in Sections 3 and 4.

Factorization theorems have recently been proven which allow one to rigorously compute certain types of exclusive B decays in terms of the light-front wavefunctions and distribution amplitudes of B meson and the final state hadrons. The proofs are similar to those used in the analysis of exclusive amplitudes involving large momentum transfer. I review this topic in Section 5 and 6.

In principle, the light-front wavefunctions contain fluctuations of states with arbitrary number of quark and gluon partons. For example, contains higher Fock states such as $uuds\bar{s}>$ and $uudc\bar{c}>$ which are intrinsic to the physics of the proton itself; *i.e.*, they are multi-connected to the valence quarks and are not generated by gluon splitting. A rigorous analysis of the momentum fraction and spin carried by intrinsic heavy quarks recently been given by Franz *et al* [25]. These quantities scale nominally as $1/m_Q^2$ in non-Abelian gauge theory, in striking contrast to the $1/m_Q^4$ scaling which follows from the Euler-Heisenberg Lagrangian in QED. In general, the intrinsic sea in the proton is asymmetric between the $Q(x)$ and $\overline{Q}(x)$ distributions, in contrast to the near symmetry of quark and antiquark distributions generated by DGLAP evolution.

The fact that the B meson contains Fock states with intrinsic strangeness and charm leads to a number of new phenomena in exclusive B decays. In particular, since the charm quarks can facilitate weak interactions, one can evade the CKM hierarchy. Susan Gardner and I have shown that the color octet intrinsic charm Fock components of the B meson can give significant modifications of standard predictions for channels such as $B \to \rho\pi$. I will review this in Section 8.

The quark and gluon probability distributions $q_i(x, Q)$ and $g(x, Q)$ of a hadron can be computed from the absolute squares of the light-front wavefunctions, integrated over the transverse momentum up to the resolution scale Q. All helicity distributions are thus encoded in terms of the light-front wavefunctions. The DGLAP evolution of the structure functions can be derived from the high $k_\perp$ properties of the light-front wavefunctions. Thus given the light-front wavefunctions, one can compute [5] all of the leading twist helicity and transversity distributions measured in polarized deep inelastic lepton scattering. For example, the helicity-specific quark distributions at resolution Λ correspond to

$$q_{\lambda_q/\Lambda_p}(x,\Lambda) = \sum_{n,q_a} \int \prod_{j=1}^{n} \frac{dx_j d^2k_{\perp j}}{16\pi^3} \sum_{\lambda_i} |\psi^{(\Lambda)}_{n/H}(x_i, \vec{k}_{\perp i}, \lambda_i)|^2 \tag{6}$$
$$\times 16\pi^3 \delta\left(1 - \sum_i^n x_i\right) \delta^{(2)}\left(\sum_i^n \vec{k}_{\perp i}\right) \delta(x - x_q)\delta_{\lambda,\lambda_q}\Theta(\Lambda^2 - \mathcal{M}_n^2) \ ,$$

where the sum is over all quarks q_a which match the quantum numbers, light-front momentum fraction x, and helicity of the struck quark. Similarly, the transversity distributions and off-diagonal helicity convolutions are defined as a density matrix of the light-front wavefunctions. This defines the LC factorization scheme [5] where the invariant mass squared $\mathcal{M}_n^2 = \sum_{i=1}^n (k_{\perp i}^2 + m_i^2)/x_i$ of the n partons of the light-front wavefunctions is limited to $\mathcal{M}_n^2 < \Lambda^2$.

However, it is not true that the leading-twist structure functions $F_i(x, Q^2)$ measured in deep inelastic lepton scattering are identical to the quark and gluon distributions. For example, it is usually assumed, following the parton model, that the F_2

structure function measured in neutral current deep inelastic lepton scattering is at leading order in $1/Q^2$ simply $F_2(x,Q^2) = \sum_q e_q^2 x q(x,Q^2)$, where $x = x_{bj} = Q^2/2p \cdot q$ and $q(x,Q)$ can be computed from the absolute square of the proton's light-front wavefunction. I will report on recent work by Paul Hoyer, Nils Marchal, Stephane Peigne, Francesco Sannino, and myself which shows that this standard identification is wrong. In particular, the shadowing corrections related to the Gribov-Glauber mechanism, the interference effects of leading twist diffractive processes in nuclei are separate effects in deep inelastic scattering, are not computable from the bound state wavefunctions of the target nucleon or nucleus.

Remarkably, it is now possible to measure the light-front wavefunctions of a relativistic hadron by diffractively dissociating it into jets whose momentum distribution is correlated with the valence quarks' momenta [26, 27, 28, 29]. At high energies each light-front Fock state interacts distinctly; *e.g.*, Fock states with small particle number and small impact separation have small color dipole moments and can traverse a nucleus with minimal interactions. This is the basis for the predictions for "color transparency" in hard quasi-exclusive [30, 31] and diffractive reactions [27, 28, 29]. QCD color transparency thus tests a fundamental ansatz of QCD, that hadronic interactions are a manifestation of gauge interactions. The E791 experiment has recently provided a remarkable confirmation of this consequence of QCD color transparency, a key property of LCWFs and the gauge field interactions in QCD. The new EVA spectrometer experiment E850 at Brookhaven has also reported striking effects of color transparency in quasi-elastic proton-proton scattering in nuclei [32]. I will review this important development in Section 7.

The CLEO collaboration has verified the scaling and angular predictions for hard exclusive two-photon processes such as $\gamma^*\gamma \to \pi^0$ and $\gamma\gamma \to \pi^+\pi^-$. The L3 experiment at LEP at CERN has also measured a number of exclusive hadron production channels in two-photon processes, providing important constraints on baryon and meson distribution amplitudes and checks of perturbative QCD factorization. These processes are particularly sensitive to the meson distribution amplitudes, the non-perturbative wavefunctions which control hard QCD exclusive processes, information essential for progress in interpreting exclusive B decays. New data from CLEO (Paar, *et al.*) for $\gamma\gamma \to \pi^+\pi^+ + K^+K^-$ at $W = \sqrt{s} > 2.5$ GeV. is in striking agreement with the perturbative QCD prediction given by Lepage and myself. Moreover, the angular distribution shows a striking transition to the predicted QCD form as W is raised. The $\gamma^*\gamma \to \pi^0$ results are in close agreement with the scaling and normalization of the PQCD prediction, provided that the pion distribution amplitude $\phi_\pi(x,Q)$ is close to the $x(1-x)$ form, the asymptotic solution to the evolution equation. In Section 6 I review the theory and emphasized the need for more such meson pair production data, particularly measurements of ratios and angular dependencies which are particularly sensitive to the meson and baryon distribution amplitudes [5], $\phi_M(x,Q)$, and $\phi_B(x_i,Q)$. These quantities specify how a hadron shares its longitudinal momentum among its valence quarks; they control virtually all exclusive processes involving a hard scale Q, including form factors, Compton scattering and photoproduction at large momentum transfer, as well as the decay of a heavy hadron into specific final states [33, 34].

The discretized light-front quantization method developed by H.C. Pauli and myself [35] is a powerful technique for finding the non-perturbative solutions of quantum field theories. The basic method is to diagonalize the light-front Hamiltonian in a light-front Fock basis defined using periodic boundary conditions in x^- and $x_\perp$. The method preserves the frame-independence of the Front form. The DLCQ method is now used extensively to solve one-space and one-time theories, including supersymmetric theories. New applications of DLCQ to supersymmetric quantum field theories and specific tests of the Maldacena conjecture have recently been given by Pinsky and Trittman.

There has been progress recently in systematically developing the computation and renormalization methods needed to make DLCQ viable for QCD in physical spacetime. Recently John Hiller, Gary McCartor and I have shown how DLCQ can be used to solve 3+1 theories despite the large numbers of degrees of freedom needed to enumerate the Fock basis [11]. A key feature of our work, is the introduction of Pauli Villars fields in order to regulate the UV divergences and perform renormalization, again while preserving the frame-independence of the theory. Further discussion will be given in Section 9. A review of DLCQ and its applications is given in Ref. [36]. There also has been important progress using the transverse lattice, essentially a combination of DLCQ in i+1 dimensions together with a lattice in the transverse space.

Models of the light-front wavefunction are important in the absence of exact solutions. A simple but potentially useful model developed by Dae Sung Hwang and myself is discussed in Section 10.

The interaction Hamiltonian of QCD in light-cone gauge can be derived by systematically applying the Dirac bracket method to identify the independent fields [37]. It contains the usual Dirac interactions between the quarks and gluons, the three-point and four-point gluon non-Abelian interactions plus instantaneous light-front-time gluon exchange and quark exchange contributions

$$\begin{aligned}
\mathcal{H}_{int} \;=\; & -g\,\overline{\psi}^i \gamma^\mu {A_\mu}^{ij} \psi^j \\
& + \frac{g}{2} f^{abc} \, (\partial_\mu {A^a}_\nu - \partial_\nu {A^a}_\mu) A^{b\mu} A^{c\nu} \\
& + \frac{g^2}{4} \, f^{abc} f^{ade} A_{b\mu} A^{d\mu} A_{c\nu} A^{e\nu} \\
& - \frac{g^2}{2} \, \overline{\psi}^i \gamma^+ \, (\gamma^{\perp'} A_{\perp'})^{ij} \, \frac{1}{i\partial_-} \, (\gamma^\perp A_\perp)^{jk} \, \psi^k
\end{aligned}$$

$$-\frac{g^2}{2}\, {j^+}_a \,\frac{1}{(\partial_-)^2}\, {j^+}_a \tag{7}$$

where

$${j^+}_a = \overline{\psi}^i \gamma^+ (t_a)^{ij} \psi^j + f_{abc}(\partial_- A_{b\mu}) A^{c\mu} \ . \tag{8}$$

In light-front time-ordered perturbation theory, a Green's functions is expanded as a power series in the interactions with light-front energy denominators $\sum_{\rm initial} k_i^- - \sum_{\rm intermediate} k_i^- + i\epsilon$ replacing the usual energy denominators. [For a review see Ref. [38].] In general each Feynman diagram with n vertices corresponds to the sum of $n!$ time-ordered contributions. However, in light-front-time-ordered perturbation theory, only those few graphs where all $k_i^+ \geq 0$ survive. In addition the form of the light-front kinetic energies is rational: $k^- = \frac{k_\perp^2 + m^2}{k^+}$, replacing the nonanalytic $k^0 = \sqrt{\vec{k}^2 + m^2}$ of equal-time theory. Thus light-front-time-ordered perturbation theory provides a viable computational method where one can trace the physical evolution of a process. The integration measures are only three-dimensional $d^2k_\perp dx$; in effect, the k^- integral of the covariant perturbation theory is performed automatically.

Alternatively, one derive Feynman rules for QCD in light-cone gauge, thus allowing the use of standard covariant computational tools and renormalization methods including dimensional regularization. Prem Srivastava and I [37] have recently presented a systematic study of light-front-quantized gauge theory in light-cone gauge using a Dyson-Wick S-matrix expansion based on light-front-time-ordered products. The gluon propagator has the form

$$\left\langle 0 \right| T({A^a}_\mu(x) {A^b}_\nu(0)) \left| 0 \right\rangle = \frac{i\delta^{ab}}{(2\pi)^4} \int d^4k \; e^{-ik\cdot x} \;\; \frac{D_{\mu\nu}(k)}{k^2 + i\epsilon} \tag{9}$$

where we have defined

$$D_{\mu\nu}(k) = D_{\nu\mu}(k) = -g_{\mu\nu} + \frac{n_\mu k_\nu + n_\nu k_\mu}{(n\cdot k)} - \frac{k^2}{(n\cdot k)^2}\, n_\mu n_\nu. \tag{10}$$

Here n_μ is a null four-vector, gauge direction, whose components are chosen to be $n_\mu = {\delta_\mu}^+,\ n^\mu = {\delta^\mu}_-$. Note also

$$\begin{aligned}
D_{\mu\lambda}(k) {D^\lambda}_\nu(k) = D_{\mu\perp}(k) {D^\perp}_\nu(k) \quad &= \quad -D_{\mu\nu}(k), \\
k^\mu D_{\mu\nu}(k) = 0, \qquad\qquad &\qquad n^\mu D_{\mu\nu}(k) \equiv D_{-\nu}(k) = 0, \\
D_{\lambda\mu}(q)\, D^{\mu\nu}(k)\, D_{\nu\rho}(q') \quad &= \quad -D_{\lambda\mu}(q) D^{\mu\rho}(q').
\end{aligned} \tag{11}$$

The gauge field propagator $\ i\, D_{\mu\nu}(k)/(k^2 + i\epsilon)\ $ is transverse not only to the gauge direction n_μ but also to k_μ, *i.e.*, it is *doubly-transverse*. This leads to appreciable simplifications in the computations in QCD. For example, the coupling of gluons to propagators carrying high momenta is automatic. The absence of collinear divergences in irreducible diagrams in the light-cone gauge greatly simplifies the leading-twist factorization of soft and hard gluonic corrections in high momentum transfer inclusive and exclusive reactions [5] since the numerators associated with the gluon coupling only have transverse components. The renormalization factors in the light-cone gauge are independent of the reference direction n^μ. Since the gluon only has physical polarization, its renormalization factors satisfy $Z_1 = Z_3$. Because of its explicit unitarity in each graph, the doubly-transverse gauge is well suited for calculations identifying the "pinch" effective charge [39, 40].

The running coupling constant and QCD β function have also been computed at one loop in the doubly-transverse light-cone gauge [37]. It is also possible to effectively quantize QCD using light-front methods in covariant Feynman gauge [41].

A remarkable advantage of light-front quantization is that the vacuum state $|\,0\rangle$ of the full QCD Hamiltonian evidently coincides with the free vacuum. The light-front vacuum is effectively trivial if the interaction Hamiltonian applied to the perturbative vacuum is zero. Note that all particles in the Hilbert space have positive energy $k^0 = \frac{1}{2}(k^+ + k^-)$, and thus positive light-front $k^\pm$. Since the plus momenta $\sum k_i^+$ is conserved by the interactions, the perturbative vacuum can only couple to states with particles in which all $k_i^+ = 0$; *i.e.*, so called zero-mode states. In the case of QED, a massive electron cannot have $k^+ = 0$ unless it also has infinite energy. In a remarkable calculation, Bassetto and collaborators [42] have shown that the computation of the spectrum of $QCD(1+1)$ in equal time quantization requires constructing the full spectrum of non perturbative contributions (instantons). In contrast, in the light-front quantization of gauge theory, where the $k^+ = 0$ singularity of the instantaneous interaction is defined by a simple infrared regularization, one obtains the correct spectrum of $QCD(1+1)$ without any need for vacuum-related contributions.

In the case of QCD(3+1), the momentum-independent four-gluon non-Abelian interaction in principle can couple the perturbative vacuum to a state with four collinear gluons in which all of the gluons have all components $k_i^\mu = 0$, thus hinting at role for zero modes in theories with massless quanta. In fact, zero modes of auxiliary fields are necessary to distinguish the theta-vacua of massless QED(1+1) [17, 43, 44], or to represent a theory in the presence of static external boundary conditions or other constraints. Zero-modes provide the light-front representation of spontaneous symmetry breaking in scalar theories [45].

There are other applications of the light-front formalism:

1. The distribution of spectator particles in the final state in the proton fragmentation region in deep inelastic scattering at an electron-proton collider are encoded in the light-front wavefunctions of the target proton. Conversely, the light-front wavefunctions can be used to describe the coalescence of comoving quarks into final state hadrons.

2. The light-front wavefunctions also specify the multi-quark and gluon correlations of the hadron. Despite the many sources of power-law corrections to the deep

inelastic cross section, certain types of dynamical contributions will stand out at large x_{bj} since they arise from compact, highly-correlated fluctuations of the proton wavefunction. In particular, there are particularly interesting dynamical $\mathcal{O}(1/Q^2)$ corrections which are due to the *interference* of quark currents; *i.e.*, contributions which involve leptons scattering amplitudes from two different quarks of the target nucleon [46].

3. The higher Fock states of the light hadrons describe the sea quark structure of the deep inelastic structure functions, including "intrinsic" strangeness and charm fluctuations specific to the hadron's structure rather than gluon substructure [47, 48]. Ladder relations connecting state of different particle number follow from the QCD equation of motion and lead to Regge behavior of the quark and gluon distributions at $x \to 0$ [49].

4. The gauge- and process-independent meson and baryon valence-quark distribution amplitudes $\phi_M(x, Q)$, and $\phi_B(x_i, Q)$ which control exclusive processes involving a hard scale Q, including heavy quark decays, are given by the valence light-front Fock state wavefunctions integrated over the transverse momentum up to the resolution scale Q. The evolution equations for distribution amplitudes follow from the perturbative high transverse momentum behavior of the light-front wavefunctions [38].

5. Proofs of factorization theorems in hard exclusive and inclusive reactions are greatly simplified since the propagating gluons in light-cone gauge couple only to transverse currents; collinear divergences are thus automatically suppressed.

6. The deuteron form factor at high Q^2 is sensitive to wavefunction configurations where all six quarks overlap within an impact separation $b_{\perp i} < \mathcal{O}(1/Q)$. The leading power-law fall off predicted by QCD is $F_d(Q^2) = f(\alpha_s(Q^2))/(Q^2)^5$, where, asymptotically, $f(\alpha_s(Q^2)) \propto \alpha_s(Q^2)^{5+2\gamma}$ [50, 51]. In general, the six-quark wavefunction of a deuteron is a mixture of five different color-singlet states. The dominant color configuration at large distances corresponds to the usual proton-neutron bound state. However at small impact space separation, all five Fock color-singlet components eventually evolve to a state with equal weight, *i.e.*, the deuteron wavefunction evolves to 80% "hidden color" [51]. The relatively large normalization of the deuteron form factor observed at large Q^2 hints at sizable hidden-color contributions [52]. Hidden color components can also play a predominant role in the reaction $\gamma d \to J/\psi pn$ at threshold if it is dominated by the multi-fusion process $\gamma gg \to J/\psi$ [53]. Hard exclusive nuclear processes can also be analyzed in terms of "reduced amplitudes" which remove the effects of nucleon substructure.

Light-front wavefunctions are thus the frame-independent interpolating functions between hadron and quark and gluon degrees of freedom. Hadron amplitudes are computed from the convolution of the light-front wavefunctions with irreducible quark-gluon amplitudes. More generally, all multi-quark and gluon correlations in the bound state are represented by the light-front wavefunctions. The light-front Fock representation is thus a representation of the underlying quantum field theory. I will discuss progress in computing light-front wavefunctions directly from QCD in Sections 9 and 10.

Light-front quantization can also be used in the Hamiltonian form to construct an event generator for high energy physics reactions at the amplitude level. The light-front partition function, summed over exponentially-weighted light-front energies, has simple boost properties which may be useful for studies in heavy ion collisions. I discuss these topics in Sections 14 and 15.

2 Other Theoretical Tools

In addition to the light-front Fock expansion, a number of other useful theoretical tools are available to eliminate theoretical ambiguities in QCD predictions:

(1) Conformal symmetry provides a template for QCD predictions [54], leading to relations between observables which are present even in a theory which is not scale invariant. For example, the natural representation of distribution amplitudes is in terms of an expansion of orthonormal conformal functions multiplied by anomalous dimensions determined by QCD evolution equations [55, 56, 57]. Thus an important guide in QCD analyses is to identify the underlying conformal relations of QCD which are manifest if we drop quark masses and effects due to the running of the QCD couplings. In fact, if QCD has an infrared fixed point (vanishing of the Gell-Mann-Low function at low momenta), the theory will closely resemble a scale-free conformally symmetric theory in many applications.

(2) Commensurate scale relations [58, 59] are perturbative QCD predictions which relate observable to observable at fixed relative scale, such as the "generalized Crewther relation" [60], which connects the Bjorken and Gross-Llewellyn Smith deep inelastic scattering sum rules to measurements of the e^+e^- annihilation cross section. Such relations have no renormalization scale or scheme ambiguity. The coefficients in the perturbative series for commensurate scale relations are identical to those of conformal QCD; thus no infrared renormalons are present [54]. One can identify the required conformal coefficients at any finite order by expanding the coefficients of the usual PQCD expansion around a formal infrared fixed point, as in the Banks-Zak method [40]. All non-conformal effects are absorbed by fixing the ratio of the respective momentum transfer and energy scales. In the case of fixed-point theories, commensurate scale relations relate both the ratio of couplings and the ratio of scales as the fixed point is approached [54].

(3) α_V and Skeleton Schemes. A physically natural scheme for defining the QCD coupling in exclusive and other processes is the $\alpha_V(Q^2)$ scheme defined from the potential of static heavy quarks. Heavy-quark lattice gauge theory can provide highly precise values for the coupling. All vacuum polarization corrections due to fermion pairs are then automatically and analytically incorporated into the Gell Mann-Low

function, thus avoiding the problem of explicitly computing and resumming quark mass corrections related to the running of the coupling [61]. The use of a finite effective charge such as α_V as the expansion parameter also provides a basis for regulating the infrared nonperturbative domain of the QCD coupling. A similar coupling and scheme can be based on an assumed skeleton expansion of the theory [39, 40].

(4) The Abelian Correspondence Principle. One can consider QCD predictions as analytic functions of the number of colors N_C and flavors N_F. In particular, one can show at all orders of perturbation theory that PQCD predictions reduce to those of an Abelian theory at $N_C \to 0$ with $\widehat{\alpha} = C_F \alpha_s$ and $\widehat{N}_F = 2N_F/C_F$ held fixed [62]. There is thus a deep connection between QCD processes and their corresponding QED analogs.

3 Applications of Light-Front Wavefunctions to Current Matrix Elements

The light-front Fock representation of current matrix elements has a number of simplifying properties. The space-like local operators for the coupling of photons, gravitons and the deep inelastic structure functions can all be expressed as overlaps of light-front wavefunctions with the same number of Fock constituents. This is possible since one can choose the special frame $q^+ = 0$ [19, 20] for space-like momentum transfer and take matrix elements of "plus" components of currents such as J^+ and T^{++}. No contributions to the current matrix elements from vacuum fluctuations occur. Similarly, given the local operators for the energy-momentum tensor $T^{\mu\nu}(x)$ and the angular momentum tensor $M^{\mu\nu\lambda}(x)$, one can directly compute momentum fractions, spin properties, and the form factors $A(q^2)$ and $B(q^2)$ appearing in the coupling of gravitons to composite systems [18].

In the case of a spin-$\frac{1}{2}$ composite system, the Dirac and Pauli form factors $F_1(q^2)$ and $F_2(q^2)$ are defined by

$$\langle P'|J^\mu(0)|P\rangle = \overline{u}(P') \left[F_1(q^2)\gamma^\mu + F_2(q^2)\frac{i}{2M}\sigma^{\mu\alpha}q_\alpha \right] u(P) \ , \tag{12}$$

where $q^\mu = (P'-P)^\mu$ and $u(P)$ is the bound state spinor. In the light-front formalism it is convenient to identify the Dirac and Pauli form factors from the helicity-conserving and helicity-flip vector current matrix elements of the J^+ current [21]:

$$\left\langle P+q,\uparrow \left| \frac{J^+(0)}{2P^+} \right| P,\uparrow \right\rangle = F_1(q^2) \ , \tag{13}$$

$$\left\langle P+q,\uparrow \left| \frac{J^+(0)}{2P^+} \right| P,\downarrow \right\rangle = -(q^1 - \mathrm{i}q^2)\frac{F_2(q^2)}{2M} \ . \tag{14}$$

The magnetic moment of a composite system is one of its most basic properties. The magnetic moment is defined at the $q^2 \to 0$ limit,

$$\mu = \frac{e}{2M}\left[F_1(0) + F_2(0)\right], \tag{15}$$

where e is the charge and M is the mass of the composite system. We use the standard light-front frame ($q^\pm = q^0 \pm q^3$):

$$\begin{aligned} q &= (q^+, q^-, \vec{q}_\perp) = \left(0, \frac{-q^2}{P^+}, \vec{q}_\perp\right), \\ P &= (P^+, P^-, \vec{P}_\perp) = \left(P^+, \frac{M^2}{P^+}, \vec{0}_\perp\right), \end{aligned} \tag{16}$$

where $q^2 = -2P\cdot q = -\vec{q}_\perp^{\,2}$ is 4-momentum square transferred by the photon.

The Pauli form factor and the anomalous magnetic moment $\kappa = \frac{e}{2M}F_2(0)$ can then be calculated from the expression

$$-(q^1 - \mathrm{i}q^2)\frac{F_2(q^2)}{2M} = \sum_a \int \frac{\mathrm{d}^2\vec{k}_\perp \mathrm{d}x}{16\pi^3} \sum_j e_j \; \psi_a^{\uparrow *}(x_i, \vec{k}'_{\perp i}, \lambda_i)\, \psi_a^{\downarrow}(x_i, \vec{k}_{\perp i}, \lambda_i) \ , \tag{17}$$

where the summation is over all contributing Fock states a and struck constituent charges e_j. The arguments of the final-state light-front wavefunction are

$$\vec{k}'_{\perp i} = \vec{k}_{\perp i} + (1 - x_i)\vec{q}_\perp \tag{18}$$

for the struck constituent and

$$\vec{k}'_{\perp i} = \vec{k}_{\perp i} - x_i\vec{q}_\perp \tag{19}$$

for each spectator. Notice that the magnetic moment must be calculated from the spin-flip non-forward matrix element of the current. In the ultra-relativistic limit where the radius of the system is small compared to its Compton scale $1/M$, the anomalous magnetic moment must vanish [21]. The light-front formalism is consistent with this theorem.

The form factors of the energy-momentum tensor for a spin-$\frac{1}{2}$ composite are defined by

$$\begin{aligned} \langle P'|T^{\mu\nu}(0)|P\rangle &= \overline{u}(P')\Big[A(q^2)\gamma^{(\mu}\overline{P}^{\nu)} + B(q^2)\frac{i}{2M}\overline{P}^{(\mu}\sigma^{\nu)\alpha}q_\alpha \\ &\qquad + C(q^2)\frac{1}{M}(q^\mu q^\nu - g^{\mu\nu}q^2)\Big]u(P) \ , \end{aligned} \tag{20}$$

where $q^\mu = (P' - P)^\mu$, $\overline{P}^\mu = \frac{1}{2}(P' + P)^\mu$, $a^{(\mu}b^{\nu)} = \frac{1}{2}(a^\mu b^\nu + a^\nu b^\mu)$, and $u(P)$ is the spinor of the system. One can also readily obtain the light-front representation of the

$A(q^2)$ and $B(q^2)$ form factors of the energy-tensor Eq. (20) [18]. In the interaction picture, only the non-interacting parts of the energy momentum tensor $T^{++}(0)$ need to be computed:

$$\left\langle P+q,\uparrow \left| \frac{T^{++}(0)}{2(P^+)^2} \right| P,\uparrow \right\rangle = A(q^2)\ , \tag{21}$$

$$\left\langle P+q,\uparrow \left| \frac{T^{++}(0)}{2(P^+)^2} \right| P,\downarrow \right\rangle = -(q^1 - \mathrm{i}q^2)\frac{B(q^2)}{2M}\ . \tag{22}$$

The $A(q^2)$ and $B(q^2)$ form factors Eqs. (21) and (22) are similar to the $F_1(q^2)$ and $F_2(q^2)$ form factors Eqs. (13) and (14) with an additional factor of the light-front momentum fraction $x = k^+/P^+$ of the struck constituent in the integrand. The $B(q^2)$ form factor is obtained from the non-forward spin-flip amplitude. The value of $B(0)$ is obtained in the $q^2 \to 0$ limit. The angular momentum projection of a state is given by

$$\begin{aligned} \left\langle J^i \right\rangle &= \frac{1}{2}\epsilon^{ijk}\int d^3x \left\langle T^{0k}x^j - T^{0j}x^k \right\rangle \\ &= A(0)\left\langle L^i \right\rangle + [A(0)+B(0)]\,\overline{u}(P)\frac{1}{2}\sigma^i u(P)\ . \end{aligned} \tag{23}$$

This result is derived using a wave-packet description of the state. The $\langle L^i \rangle$ term is the orbital angular momentum of the center of mass motion with respect to an arbitrary origin and can be dropped. The coefficient of the $\langle L^i \rangle$ term must be 1; $A(0) = 1$ also follows when we evaluate the four-momentum expectation value $\langle P^\mu \rangle$. Thus the total intrinsic angular momentum J^z of a nucleon can be identified with the values of the form factors $A(q^2)$ and $B(q^2)$ at $q^2 = 0$:

$$\langle J^z \rangle = \left\langle \frac{1}{2}\sigma^z \right\rangle [A(0)+B(0)]\ . \tag{24}$$

The anomalous moment coupling $B(0)$ to a graviton can in fact be shown to vanish for any composite system. This remarkable result, first derived by Okun and Kobzarev [63, 64, 65, 66, 67], follows directly from the Lorentz boost properties of the light-front Fock representation [18].

Dae Sung Hwang, Bo-Qiang Ma, Ivan Schmidt, and I [18] have recently shown that the light-front wavefunctions generated by the radiative corrections to the electron in QED provides a simple system for understanding the spin and angular momentum decomposition of relativistic systems. This perturbative model also illustrates the interconnections between Fock states of different number. The model is patterned after the quantum structure which occurs in the one-loop Schwinger $\alpha/2\pi$ correction to the electron magnetic moment [21]. In effect, we can represent a spin-$\frac{1}{2}$ system as a composite of a spin-$\frac{1}{2}$ fermion and spin-one vector boson with arbitrary masses. A

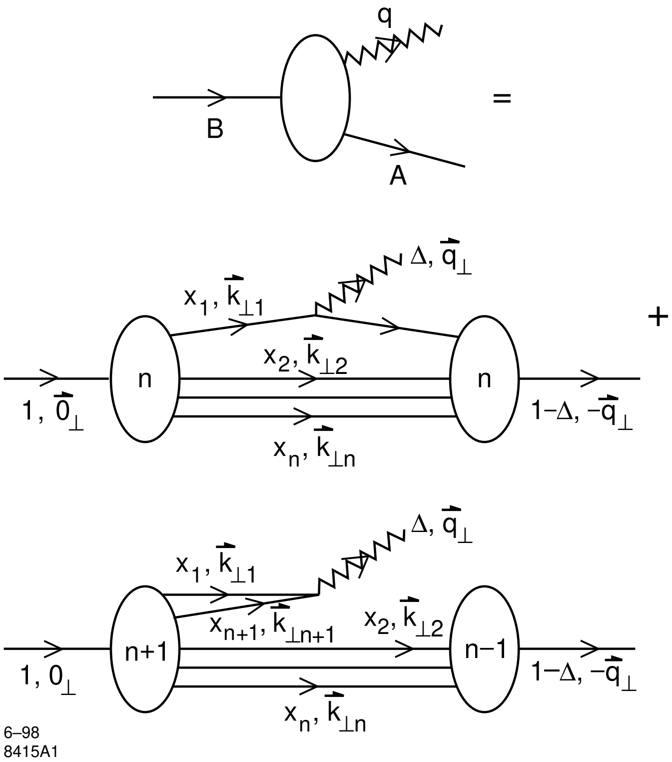

Figure 3: Exact representation of electroweak decays and time-like form factors in the light-front Fock representation.

similar model has been used to illustrate the matrix elements and evolution of light-front helicity and orbital angular momentum operators [68]. This representation of a composite system is particularly useful because it is based on two constituents but yet is totally relativistic. We can then explicitly compute the form factors $F_1(q^2)$ and $F_2(q^2)$ of the electromagnetic current, and the various contributions to the form factors $A(q^2)$ and $B(q^2)$ of the energy-momentum tensor.

Another remarkable advantage of the light-front formalism is that exclusive semileptonic B-decay amplitudes such as $B \to A\ell\overline{\nu}$ can also be evaluated exactly [22]. The time-like decay matrix elements require the computation of the diagonal matrix element $n \to n$ where parton number is conserved, and the off-diagonal $n+1 \to n-1$ convolution where the current operator annihilates a $q\overline{q'}$ pair in the initial B wavefunction. See Fig. 3. This term is a consequence of the fact that the time-like decay $q^2 = (p_\ell + p_{\overline{\nu}})^2 > 0$ requires a positive light-front momentum fraction $q^+ > 0$. Conversely for space-like currents, one can choose $q^+ = 0$, as in the Drell-Yan-West representation of the space-like electromagnetic form factors. However, as can be seen from the explicit analysis of the form factor in a perturbative model, the off-diagonal convolution can yield a nonzero q^+/q^+ limiting form as $q^+ \to 0$. This extra term appears specifically in the case of "bad" currents such as J^- in which the coupling to $q\overline{q}$ fluctuations in the light-front wavefunctions are favored. In effect, the $q^+ \to 0$ limit generates $\delta(x)$ contributions as residues of the $n+1 \to n-1$ contributions. The necessity for such "zero mode" $\delta(x)$ terms has been noted by Chang, Root and Yan [69], Burkardt [70], and Ji and Choi [71].

The off-diagonal $n+1 \to n-1$ contributions give a new perspective for the physics of B-decays. A semileptonic decay involves not only matrix elements where a quark changes flavor, but also a contribution where the leptonic pair is created from the annihilation of a $q\overline{q'}$ pair within the Fock states of the initial B wavefunction. The semileptonic decay thus can occur from the annihilation of a nonvalence quark-antiquark pair in the initial hadron. This feature will carry over to exclusive hadronic B-decays, such as $B^0 \to \pi^- D^+$. In this case the pion can be produced from the coalescence of a $d\overline{u}$ pair emerging from the initial higher particle number Fock wavefunction of the B. The D meson is then formed from the remaining quarks after the internal exchange of a W boson.

In principle, a precise evaluation of the hadronic matrix elements needed for B-decays and other exclusive electroweak decay amplitudes requires knowledge of all of the light-front Fock wavefunctions of the initial and final state hadrons. In the case of model gauge theories such as QCD(1+1) [72] or collinear QCD [73] in one-space and one-time dimensions, the complete evaluation of the light-front wavefunction is possible for each baryon or meson bound-state using the DLCQ method. It would be interesting to use such solutions as a model for physical B-decays.

4 Light-front Representation of Deeply Virtual Compton Scattering

The virtual Compton scattering process $\frac{d\sigma}{dt}(\gamma^* p \to \gamma p)$ for large initial photon virtuality $q^2 = -Q^2$ has extraordinary sensitivity to fundamental features of the proton's structure. Even though the final state photon is on-shell, the deeply virtual process probes the elementary quark structure of the proton near the light front as an effective local current. In contrast to deep inelastic scattering, which measures only the absorptive part of the forward virtual Compton amplitude $Im\mathcal{T}_{\gamma^* p \to \gamma^* p}$, deeply virtual Compton scattering allows the measurement of the phase and spin structure of proton matrix elements for general momentum transfer squared t. In addition, the interference of the virtual Compton amplitude and Bethe-Heitler wide angle scattering Bremsstrahlung amplitude where the photon is emitted from the lepton line leads to an electron-positron asymmetry in the $e^\pm p \to e^\pm \gamma p$ cross section which is proportional to the real part of the Compton amplitude [74, 75, 76]. The deeply virtual Compton amplitude $\gamma^* p \to \gamma p$ is related by crossing to another important process

$\gamma^*\gamma \to$ hadron pairs at fixed invariant mass which can be measured in electron-photon collisions [77].

To leading order in $1/Q$, the deeply virtual Compton scattering amplitude $\gamma^*(q)p(P) \to \gamma(q')p(P')$ factorizes as the convolution in x of the amplitude $t^{\mu\nu}$ for hard Compton scattering on a quark line with the generalized Compton form factors $H(x,t,\zeta)$, $E(x,t,\zeta)$, $\tilde{H}(x,t,\zeta)$, and $\tilde{E}(x,t,\zeta)$ of the target proton [64, 65, 78, 79, 80, 81, 82, 83, 84, 85, 86, 87]. Here x is the light-front momentum fraction of the struck quark, and $\zeta = Q^2/2P\cdot q$ plays the role of the Bjorken variable. The square of the four-momentum transfer from the proton is given by $t = \Delta^2 \; = \; 2P{\cdot}\Delta \; = \; -\frac{(\zeta^2 M^2 + \vec{\Delta}_\perp^2)}{(1-\zeta)}$, where Δ is the difference of initial and final momenta of the proton ($P = P' + \Delta$). We will be interested in deeply virtual Compton scattering where q^2 is large compared to the masses and t. Then, to leading order in $1/Q^2$, $\frac{-q^2}{2P_I\cdot q} = \zeta$. Thus ζ plays the role of the Bjorken variable in deeply virtual Compton scattering. For a fixed value of $-t$, the allowed range of ζ is given by

$$0 \;\le\; \zeta \;\le\; \frac{(-t)}{2M^2}\;\left(\sqrt{1+\frac{4M^2}{(-t)}}\;-\;1\right)\;. \tag{25}$$

The form factor $H(x,t,\zeta)$ describes the proton response when the helicity of the proton is unchanged, and $E(x,t,\zeta)$ is for the case when the proton helicity is flipped. Two additional functions $\tilde{H}(x,t,\zeta)$, and $\tilde{E}(x,t,\zeta)$ appear, corresponding to the dependence of the Compton amplitude on quark helicity.

Recently, Markus Diehl, Dae Sung Hwang and I [23] have shown how the deeply virtual Compton amplitude can be evaluated explicitly in the Fock state representation using the matrix elements of the currents and the boost properties of the light-front wavefunctions. For the $n \to n$ diagonal term ($\Delta n = 0$), the arguments of the final-state hadron wavefunction are $\frac{x_1-\zeta}{1-\zeta}$, $\vec{k}_{\perp 1} - \frac{1-x_1}{1-\zeta}\vec{\Delta}_\perp$ for the struck quark and $\frac{x_i}{1-\zeta}$, $\vec{k}_{\perp i} + \frac{x_i}{1-\zeta}\vec{\Delta}_\perp$ for the $n-1$ spectators. We thus obtain formulae for the diagonal (parton-number-conserving) contribution to the generalized form factors for deeply virtual Compton amplitude in the domain [85, 84, 88] $\zeta \le x_1 \le 1$:

$$\begin{aligned}
& \sqrt{1-\zeta} f_{1\,(n\to n)}(x_1,t,\zeta) \;-\; \frac{\zeta^2}{4\sqrt{1-\zeta}} f_{2\,(n\to n)}(x_1,t,\zeta) \\
=\; & \sum_{n,\ \lambda}\prod_{i=1}^{n}\int_0^1 dx_{i(i\neq 1)}\int\frac{d^2\vec{k}_{\perp i}}{2(2\pi)^3}\;\delta\left(1-\sum_{j=1}^{n}x_j\right)\;\delta^{(2)}\left(\sum_{j=1}^{n}\vec{k}_{\perp j}\right) \\
& \times\psi^{\uparrow\,*}_{(n)}(x'_i,\vec{k}'_{\perp i},\lambda_i)\;\psi^{\uparrow}_{(n)}(x_i,\vec{k}_{\perp i},\lambda_i)(\sqrt{1-\zeta})^{1-n},
\end{aligned} \tag{26}$$

$$\sqrt{1-\zeta}\;\left(1+\frac{\zeta}{2(1-\zeta)}\right)\;\frac{(\Delta^1 - \mathrm{i}\Delta^2)}{2M} f_{2\,(n\to n)}(x_1,t,\zeta)$$

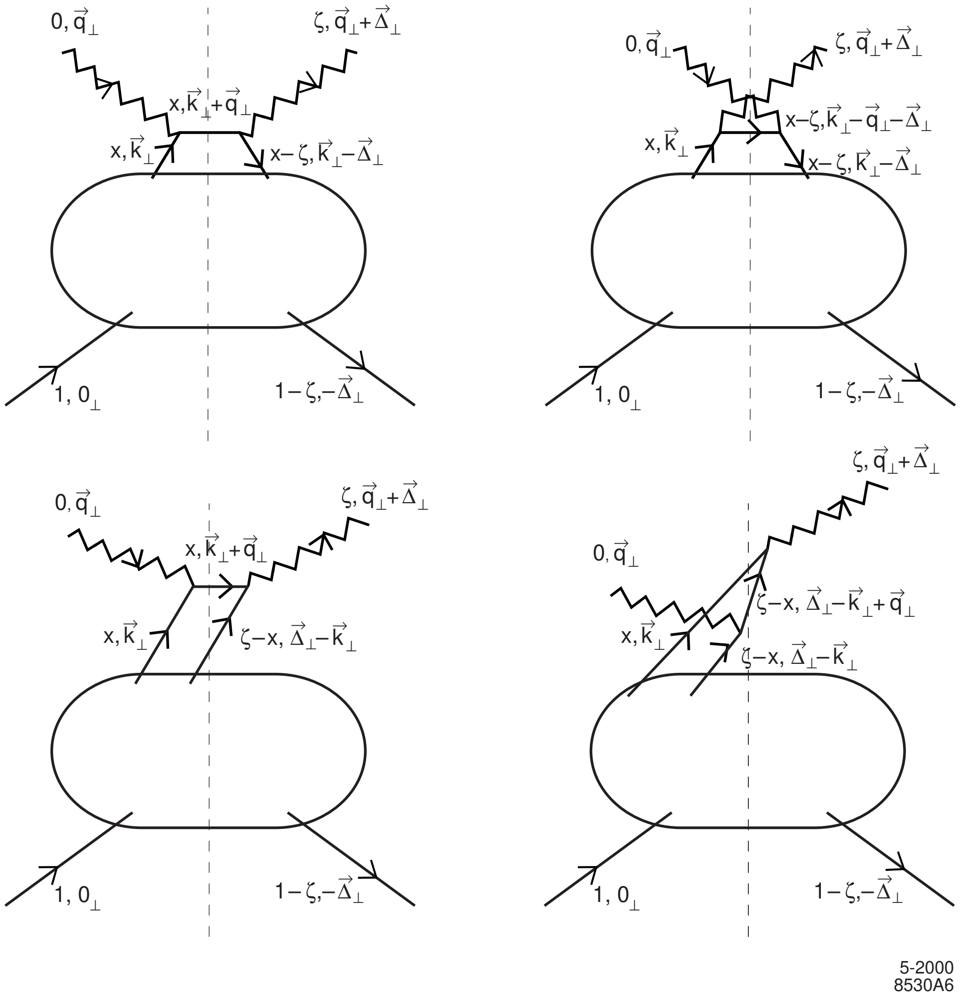

Figure 4: Light-front time-ordered contributions to deeply virtual Compton scattering. Only the contributions of leading twist in $1/q^2$ are illustrated. These contributions illustrate the factorization property of the leading twist amplitude.

$$= \sum_{n,\ \lambda} \prod_{i=1}^{n} \int_0^1 dx_{i(i\neq 1)} \int \frac{d^2\vec{k}_{\perp i}}{2(2\pi)^3}\ \delta\left(1-\sum_{j=1}^{n} x_j\right)\ \delta^{(2)}\left(\sum_{j=1}^{n} \vec{k}_{\perp j}\right)$$

$$\times \psi^{\uparrow\, *}_{(n)}(x'_i, \vec{k}'_{\perp i}, \lambda_i)\ \psi^{\downarrow}_{(n)}(x_i, \vec{k}_{\perp i}, \lambda_i)(\sqrt{1-\zeta})^{1-n}, \tag{27}$$

where

$$\begin{cases} x'_1 = \frac{x_1-\zeta}{1-\zeta}\,, & \vec{k}'_{\perp 1} = \vec{k}_{\perp 1} - \frac{1-x_1}{1-\zeta}\vec{\Delta}_\perp \quad \text{for the struck quark,} \\ x'_i = \frac{x_i}{1-\zeta}\,, & \vec{k}'_{\perp i} = \vec{k}_{\perp i} + \frac{x_i}{1-\zeta}\vec{\Delta}_\perp \quad \text{for the } (n-1) \text{ spectators.} \end{cases} \tag{28}$$

A sum over all possible helicities λ_i is understood. If quark masses are neglected, the currents conserve helicity. We also can check that $\sum_{i=1}^{n} x'_i = 1$, $\sum_{i=1}^{n} \vec{k}'_{\perp i} = \vec{0}_\perp$.

For the $n+1 \to n-1$ off-diagonal term ($\Delta n = -2$), consider the case where partons 1 and $n+1$ of the initial wavefunction annihilate into the current leaving $n-1$ spectators. Then $x_{n+1} = \zeta - x_1$, $\vec{k}_{\perp n+1} = \vec{\Delta}_\perp - \vec{k}_{\perp 1}$. The remaining $n-1$ partons have total momentum $((1-\zeta)P^+, -\vec{\Delta}_\perp)$. The final wavefunction then has arguments $x'_i = \frac{x_i}{1-\zeta}$ and $\vec{k}'_{\perp i} = \vec{k}_{\perp i} + \frac{x_i}{1-\zeta}\vec{\Delta}_\perp$. We thus obtain the formulae for the off-diagonal matrix element of the Compton amplitude in the domain $0 \le x_1 \le \zeta$:

$$\sqrt{1-\zeta} f_{1\,(n+1\to n-1)}(x_1,t,\zeta)\ -\ \frac{\zeta^2}{4\sqrt{1-\zeta}} f_{2\,(n+1\to n-1)}(x_1,t,\zeta)$$

$$= \sum_{n,\ \lambda} \int_0^1 dx_{n+1} \int \frac{d^2\vec{k}_{\perp 1}}{2(2\pi)^3} \int \frac{d^2\vec{k}_{\perp n+1}}{2(2\pi)^3} \prod_{i=2}^{n} \int_0^1 dx_i \int \frac{d^2\vec{k}_{\perp i}}{2(2\pi)^3}$$

$$\times \delta\left(1-\sum_{j=1}^{n+1} x_j\right)\ \delta^{(2)}\left(\sum_{j=1}^{n+1} \vec{k}_{\perp j}\right) [\sqrt{1-\zeta}]^{1-n}$$

$$\times \psi^{\uparrow\, *}_{(n-1)}(x'_i, \vec{k}'_{\perp i}, \lambda_i)\ \psi^{\uparrow}_{(n+1)}(\{x_1, x_i, x_{n+1} = \zeta - x_1\},$$

$$\{\vec{k}_{\perp 1}, \vec{k}_{\perp i}, \vec{k}_{\perp n+1} = \vec{\Delta}_\perp - \vec{k}_{\perp 1}\}, \{\lambda_1, \lambda_i, \lambda_{n+1} = -\lambda_1\}), \tag{29}$$

$$\sqrt{1-\zeta}\left(1+\frac{\zeta}{2(1-\zeta)}\right)\frac{(\Delta^1 - \mathrm{i}\Delta^2)}{2M} f_{2\,(n+1\to n-1)}(x_1,t,\zeta)$$

$$= \sum_{n,\ \lambda} \int_0^1 dx_{n+1} \int \frac{d^2\vec{k}_{\perp 1}}{2(2\pi)^3} \int \frac{d^2\vec{k}_{\perp n+1}}{2(2\pi)^3} \prod_{i=2}^{n} \int_0^1 dx_i \int \frac{d^2\vec{k}_{\perp i}}{2(2\pi)^3}$$

$$\times \delta\left(1-\sum_{j=1}^{n+1} x_j\right)\ \delta^{(2)}\left(\sum_{j=1}^{n+1} \vec{k}_{\perp j}\right) [\sqrt{1-\zeta}]^{1-n}$$

$$\times\psi^{\uparrow\,*}_{(n-1)}(x'_i, \vec{k}'_{\perp i}, \lambda_i)\ \psi^{\downarrow}_{(n+1)}(\{x_1, x_i, x_{n+1} = \zeta - x_1\},$$

$$\{\vec{k}_{\perp 1}, \vec{k}_{\perp i}, \vec{k}_{\perp n+1} = \vec{\Delta}_\perp - \vec{k}_{\perp 1}\}, \{\lambda_1, \lambda_i, \lambda_{n+1} = -\lambda_1\}), \qquad (30)$$

where $i = 2, 3, \cdots, n$ label the $n-1$ spectator partons which appear in the final-state hadron wavefunction with

$$x'_i = \frac{x_i}{1-\zeta}\,, \qquad \vec{k}'_{\perp i} = \vec{k}_{\perp i} + \frac{x_i}{1-\zeta}\vec{\Delta}_\perp\ . \qquad (31)$$

We can again check that the arguments of the final-state wavefunction satisfy $\sum_{i=2}^{n} x'_i = 1$, $\sum_{i=2}^{n} \vec{k}'_{\perp i} = \vec{0}_\perp$.

The above representation is the general form for the generalized form factors of the deeply virtual Compton amplitude for any composite system. Thus given the light-front Fock state wavefunctions of the eigensolutions of the light-front Hamiltonian, we can compute the amplitude for virtual Compton scattering including all spin correlations. The formulae are accurate to leading order in $1/Q^2$. Radiative corrections to the quark Compton amplitude of order $\alpha_s(Q^2)$ from diagrams in which a hard gluon interacts between the two photons have also been neglected.

5 Applications of QCD Factorization to Hard QCD Processes

Factorization theorems for hard exclusive, semi-exclusive, and diffractive processes allow the separation of soft non-perturbative dynamics of the bound state hadrons from the hard dynamics of a perturbatively-calculable quark-gluon scattering amplitude. The factorization of inclusive reactions is reviewed in ref. For reviews and bibliography of exclusive process calculations in QCD (see Ref. [38, 89]).

The light-front formalism provides a physical factorization scheme which conveniently separates and factorizes soft non-perturbative physics from hard perturbative dynamics in both exclusive and inclusive reactions [5, 90].

In hard inclusive reactions all intermediate states are divided according to $\mathcal{M}^2_n < \Lambda^2$ and $\mathcal{M}^2_n > \Lambda^2$ domains. The lower mass regime is associated with the quark and gluon distributions defined from the absolute squares of the LC wavefunctions in the light front factorization scheme. In the high invariant mass regime, intrinsic transverse momenta can be ignored, so that the structure of the process at leading power has the form of hard scattering on collinear quark and gluon constituents, as in the parton model. The attachment of gluons from the LC wavefunction to a propagator in a hard subprocess is power-law suppressed in LC gauge, so that the minimal quark-gluon particle-number subprocesses dominate. It is then straightforward to derive the DGLAP equations from the evolution of the distributions with $\log \Lambda^2$. The anomaly contribution to singlet helicity structure function $g_1(x, Q)$ can be explicitly identified in the LC factorization scheme as due to the $\gamma^* g \to q\overline{q}$ fusion process. The anomaly contribution would be zero if the gluon is on shell. However, if the off-shellness of the state is larger than the quark pair mass, one obtains the usual anomaly contribution [91].

In exclusive amplitudes, the LC wavefunctions are the interpolating amplitudes connecting the quark and gluons to the hadronic states. In an exclusive amplitude involving a hard scale Q^2 all intermediate states can be divided according to $\mathcal{M}_n^2 < \Lambda^2 < Q^2$ and $\mathcal{M}_n^2 < \Lambda^2$ invariant mass domains. The high invariant mass contributions to the amplitude has the structure of a hard scattering process T_H in which the hadrons are replaced by their respective (collinear) quarks and gluons. In light-cone gauge only the minimal Fock states contribute to the leading power-law fall-off of the exclusive amplitude. The wavefunctions in the lower invariant mass domain can be integrated up to an arbitrary intermediate invariant mass cutoff Λ. The invariant mass domain beyond this cutoff is included in the hard scattering amplitude T_H. The T_H satisfy dimensional counting rules [92]. Final-state and initial state corrections from gluon attachments to lines connected to the color-singlet distribution amplitudes cancel at leading twist. Explicit examples of perturbative QCD factorization will be discussed in more detail in the next section.

The key non-perturbative input for exclusive processes is thus the gauge and frame independent hadron distribution amplitude [90, 5] defined as the integral of the valence (lowest particle number) Fock wavefunction; *e.g.* for the pion

$$\phi_\pi(x_i, \Lambda) \equiv \int d^2k_\perp \, \psi^{(\Lambda)}_{q\overline{q}/\pi}(x_i, \vec{k}_{\perp i}, \lambda) \tag{32}$$

where the global cutoff Λ is identified with the resolution Q. The distribution amplitude controls leading-twist exclusive amplitudes at high momentum transfer, and it can be related to the gauge-invariant Bethe-Salpeter wavefunction at equal light-front time. The logarithmic evolution of hadron distribution amplitudes $\phi_H(x_i, Q)$ can be derived from the perturbatively-computable tail of the valence light-front wavefunction in the high transverse momentum regime [90, 5]. The conformal basis for the evolution of the three-quark distribution amplitudes for the baryons [93] has recently been obtained by V. Braun *et al.*[57].

The existence of an exact formalism provides a basis for systematic approximations and a control over neglected terms. For example, one can analyze exclusive semi-leptonic B-decays which involve hard internal momentum transfer using a perturbative QCD formalism [94, 95, 33, 34, 96, 97] patterned after the perturbative analysis of form factors at large momentum transfer. The hard-scattering analysis again proceeds by writing each hadronic wavefunction as a sum of soft and hard contributions

$$\psi_n = \psi_n^{\rm soft}(\mathcal{M}_n^2 < \Lambda^2) + \psi_n^{\rm hard}(\mathcal{M}_n^2 > \Lambda^2), \tag{33}$$

where $\mathcal{M}_n^2$ is the invariant mass of the partons in the n-particle Fock state and Λ is the separation scale. The high internal momentum contributions to the wavefunction $\psi_n^{\rm hard}$ can be calculated systematically from QCD perturbation theory by iterating the gluon exchange kernel. The contributions from high momentum transfer exchange to the B-decay amplitude can then be written as a convolution of a hard-scattering quark-gluon scattering amplitude T_H with the distribution amplitudes $\phi(x_i, \Lambda)$, the valence wavefunctions obtained by integrating the constituent momenta up to the separation scale $\mathcal{M}_n < \Lambda < Q$. Furthermore in processes such as $B \to \pi D$ where the pion is effectively produced as a rapidly-moving small Fock state with a small color-dipole interactions, final state interactions are suppressed by color transparency. This is the basis for the perturbative hard-scattering analyses [94, 33, 34, 96, 97]. In a systematic analysis, one can identify the hard PQCD contribution as well as the soft contribution from the convolution of the light-front wavefunctions. Furthermore, the hard-scattering contribution can be systematically improved.

Given the solution for the hadronic wavefunctions $\psi_n^{(\Lambda)}$ with $\mathcal{M}_n^2 < \Lambda^2$, one can construct the wavefunction in the hard regime with $\mathcal{M}_n^2 > \Lambda^2$ using projection operator techniques. The construction can be done perturbatively in QCD since only high invariant mass, far off-shell matrix elements are involved. One can use this method to derive the physical properties of the LC wavefunctions and their matrix elements at high invariant mass. Since $\mathcal{M}_n^2 = \sum_{i=1}^n \left(\frac{k_\perp^2+m^2}{x}\right)_i$, this method also allows the derivation of the asymptotic behavior of light-front wavefunctions at large $k_\perp$, which in turn leads to predictions for the fall-off of form factors and other exclusive matrix elements at large momentum transfer, such as the quark counting rules for predicting the nominal power-law fall-off of two-body scattering amplitudes at fixed θ_{cm} [92] and helicity selection rules [98]. The phenomenological successes of these rules can be understood within QCD if the coupling $\alpha_V(Q)$ freezes in a range of relatively small momentum transfer [99].

6 Two-Photon Processes

The simplest and perhaps the most elegant illustration of an exclusive reaction in QCD is the evaluation of the photon-to-pion transition form factor $F_{\gamma\to\pi}(Q^2)$ [5, 100] which is measurable in single-tagged two-photon $ee \to ee\pi^0$ reactions. The form factor is defined via the invariant amplitude $\Gamma^\mu = -ie^2 F_{\pi\gamma}(Q^2)\epsilon^{\mu\nu\rho\sigma}p_\nu^\pi \epsilon_\rho q_\sigma$. As in inclusive reactions, one must specify a factorization scheme which divides the integration regions of the loop integrals into hard and soft momenta, compared to the resolution scale $\tilde{Q}$. At leading twist, the transition form factor then factorizes as a convolution of the $\gamma^*\gamma \to q\overline{q}$ amplitude (where the quarks are collinear with the final

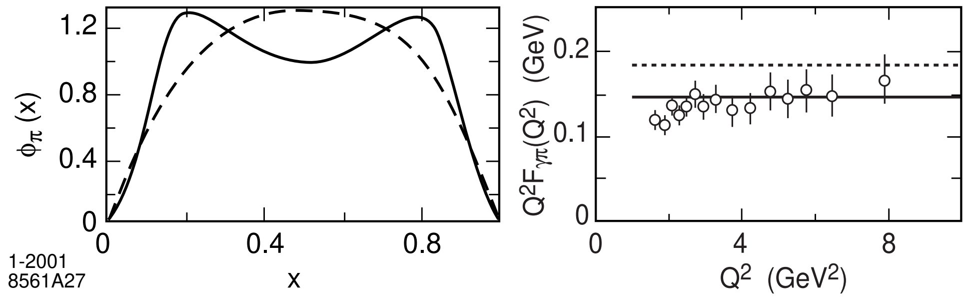

Figure 5: (a) Preliminary transverse lattice results for the pion distribution amplitude at $Q^2 \sim 10$ GeV^2. The solid curve is the theoretical prediction from the combined DLCQ/transverse lattice method [107]; the chain line is the experimental result obtained from jet diffractive dissociation [26]. Both are normalized to the same area for comparison. (b) Scaling of the transition photon to pion transition form factor $Q^2F_{\gamma\pi^0}(Q^2)$. The dotted and solid theoretical curves are the perturbative QCD prediction at leading and next-to-leading order, respectively, assuming the asymptotic pion distribution The data are from the CLEO collaboration [102].

state pion) with the valence light-front wavefunction of the pion:

$$F_{\gamma M}(Q^2) = \frac{4}{\sqrt{3}} \int_0^1 dx \phi_M(x, \tilde{Q}) T^H_{\gamma \to M}(x, Q^2). \tag{34}$$

The hard scattering amplitude for $\gamma\gamma^* \to q\overline{q}$ is $T^H_{\gamma M}(x, Q^2) = [(1-x)Q^2]^{-1} \times (1 + \mathcal{O}(\alpha_s))$. The leading QCD corrections have been computed by Braaten [101]. The evaluation of the next-to-leading corrections in the physical α_V scheme is given in Ref. [99]. For the asymptotic distribution amplitude $\phi^{\rm asympt}_\pi(x) = \sqrt{3} f_\pi x(1-x)$ one predicts $Q^2F_{\gamma\pi}(Q^2) = 2f_\pi \left(1 - \frac{5}{3}\frac{\alpha_V(Q^*)}{\pi}\right)$ where $Q^* = e^{-3/2}Q$ is the BLM scale for the pion form factor. The PQCD predictions have been tested in measurements of $e\gamma \to e\pi^0$ by the CLEO collaboration [102]. See Fig. 5 (b). The observed flat scaling of the $Q^2F_{\gamma\pi}(Q^2)$ data from $Q^2 = 2$ to $Q^2 = 8$ GeV^2 provides an important confirmation of the applicability of leading twist QCD to this process. The magnitude of $Q^2F_{\gamma\pi}(Q^2)$ is remarkably consistent with the predicted form, assuming the asymptotic distribution amplitude and including the LO QCD radiative correction with $\alpha_V(e^{-3/2}Q)/\pi \simeq 0.12$. One could allow for some broadening of the distribution amplitude with a corresponding increase in the value of α_V at small scales. Radyushkin [103], Ong [104], and Kroll [105] have also noted that the scaling and normalization of the photon-to-pion transition form factor tends to favor the asymptotic form for the pion distribution amplitude and rules out broader distributions such as the two-humped form suggested by QCD sum rules [106].

The two-photon annihilation process $\gamma^*\gamma \to$ hadrons, which is measurable in single-tagged $e^+e^- \to e^+e^-$hadrons events, provides a semi-local probe of $C = +$

hadron systems $\pi^0, \eta^0, \eta', \eta_c, \pi^+\pi^-$, etc. The $\gamma^*\gamma \to \pi^+\pi^-$ hadron pair process is related to virtual Compton scattering on a pion target by crossing. The leading twist amplitude is sensitive to the $1/x - 1/(1-x)$ moment of the two-pion distribution amplitude coupled to two valence quarks [88, 77].

Two-photon reactions, $\gamma\gamma \to H\overline{H}$ at large s $= (k_1 + k_2)^2$ and fixed $\theta_{\rm cm}$, provide a particularly important laboratory for testing QCD since these cross-channel "Compton" processes are the simplest calculable large-angle exclusive hadronic scattering reactions. The helicity structure, and often even the absolute normalization can be rigorously computed for each two-photon channel [100]. In the case of meson pairs, dimensional counting predicts that for large s, $s^4 d\sigma/dt(\gamma\gamma \to M\overline{M}$ scales at fixed t/s or $\theta_{\rm c.m.}$ up to factors of $\ln s/\Lambda^2$. The angular dependence of the $\gamma\gamma \to H\overline{H}$ amplitudes can be used to determine the shape of the process-independent distribution amplitudes, $\phi_H(x,Q)$. An important feature of the $\gamma\gamma \to M\overline{M}$ amplitude for meson pairs is that the contributions of Landshoff pitch singularities are power-law suppressed at the Born level—even before taking into account Sudakov form factor suppression. There are also no anomalous contributions from the $x \to 1$ endpoint integration region. Thus, as in the calculation of the meson form factors, each fixed-angle helicity amplitude can be written to leading order in $1/Q$ in the factorized form $[Q^2 = p_T^2 = tu/s; \tilde{Q}_x = \min(xQ, (l-x)Q)]$:

$$\mathcal{M}_{\gamma\gamma\to M\overline{M}} = \int_0^1 dx \int_0^1 dy \phi_{\overline{M}}(y, \tilde{Q}_y) T_H(x, y, s, \theta_{\rm c.m.} \phi_M(x, \tilde{Q}_x), \tag{35}$$

where T_H is the hard-scattering amplitude $\gamma\gamma \to (q\overline{q})(q\overline{q})$ for the production of the valence quarks collinear with each meson, and $\phi_M(x, \tilde{Q})$ is the amplitude for finding the valence q and $\overline{q}$ with light-front fractions of the meson's momentum, integrated over transverse momenta $k_\perp < \tilde{Q}$. The contribution of non-valence Fock states are power-law suppressed. Furthermore, the helicity-selection rules [98] of perturbative QCD predict that vector mesons are produced with opposite helicities to leading order in $1/Q$ and all orders in α_s. The dependence in x and y of several terms in $T_{\lambda,\lambda'}$ is quite similar to that appearing in the meson's electromagnetic form factor. Thus much of the dependence on $\phi_M(x,Q)$ can be eliminated by expressing it in terms of the meson form factor. In fact, the ratio of the $\gamma\gamma \to \pi^+\pi^-$ and $e^+e^- \to \mu^+\mu^-$ amplitudes at large s and fixed θ_{CM} is nearly insensitive to the running coupling and the shape of the pion distribution amplitude:

$$\frac{\frac{d\sigma}{dt}(\gamma\gamma \to \pi^+\pi^-)}{\frac{d\sigma}{dt}(\gamma\gamma \to \mu^+\mu^-)} \sim \frac{4|F_\pi(s)|^2}{1 - \cos^2\theta_{\rm c.m.}}. \tag{36}$$

The comparison of the PQCD prediction for the sum of $\pi^+\pi^-$ plus K^+K^- channels with recent CLEO data [108] is shown in Fig. 6. The CLEO data for charged pion and kaon pairs show a clear transition to the scaling and angular distribution predicted by PQCD [100] for $W = \sqrt{(s_{\gamma\gamma}} > 2$ GeV. See Fig. 6. It is clearly important to measure

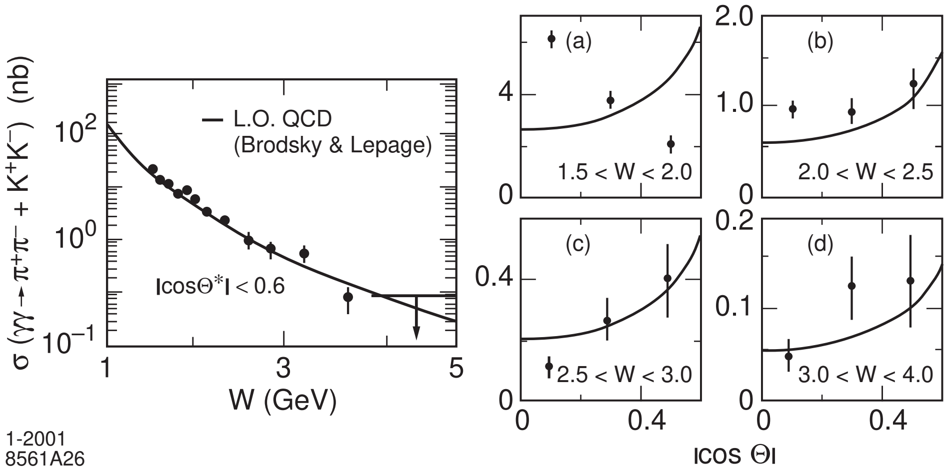

Figure 6: Comparison of the sum of $\gamma\gamma \to \pi^+\pi^-$ and $\gamma\gamma \to K^+K^-$ meson pair production cross sections with the scaling and angular distribution of the perturbative QCD prediction [100]. The data are from the CLEO collaboration [108].

the magnitude and angular dependence of the two-photon production of neutral pions and $\rho^+\rho^-$ cross sections in view of the strong sensitivity of these channels to the shape of meson distribution amplitudes. QCD also predicts that the production cross section for charged ρ-pairs (with any helicity) is much larger that for that of neutral ρ pairs, particularly at large $\theta_{\rm c.m.}$ angles. Similar predictions are possible for other helicity-zero mesons. The cross sections for Compton scattering on protons and the crossed reaction $\gamma\gamma \to p\overline{p}$ at high momentum transfer have also been evaluated [109, 110], providing important tests of the proton distribution amplitude.

It is particularly compelling to see a transition in angular dependence between the low energy chiral and PQCD regimes. The success of leading-twist perturbative QCD scaling for exclusive processes at presently experimentally accessible momentum transfer can be understood if the effective coupling $\alpha_V(Q^*)$ is approximately constant at the relatively small scales Q^* relevant to the hard scattering amplitudes [99]. The evolution of the quark distribution amplitudes In the low-Q^* domain at also needs to be minimal. Sudakov suppression of the endpoint contributions is also strengthened if the coupling is frozen because of the exponentiation of a double logarithmic series.

A debate has continued [111, 112, 113, 114] on whether processes such as the pion and proton form factors and elastic Compton scattering $\gamma p \to \gamma p$ might be dominated by higher-twist mechanisms until very large momentum transfer. If one assumes that the light-front wavefunction of the pion has the form $\psi_{\rm soft}(x, k_\perp) = A \exp(-b\frac{k_\perp^2}{x(1-x)})$, then the Feynman endpoint contribution to the overlap integral at small $k_\perp$ and $x \simeq 1$ will dominate the form factor compared to the hard-scattering contribution until very large Q^2. However, this ansatz for $\psi_{\rm soft}(x, k_\perp)$ has no suppression at $k_\perp = 0$ for any x; *i.e.*, the wavefunction in the hadron rest frame does not fall-off at all for $k_\perp = 0$ and $k_z \to -\infty$. Thus such wavefunctions do not represent well soft QCD contributions. Endpoint contributions are also suppressed by the QCD Sudakov form factor, reflecting the fact that a near-on-shell quark must radiate if it absorbs large momentum. One can show [5] that the leading power dependence of the two-particle light-front Fock wavefunction in the endpoint region is $1-x$, giving a meson structure function which falls as $(1-x)^2$ and thus by duality a non-leading contribution to the meson form factor $F(Q^2) \propto 1/Q^3$. Thus the dominant contribution to meson form factors comes from the hard-scattering regime.

Radyushkin [112] has argued that the Compton amplitude is dominated by soft end-point contributions of the proton wavefunctions where the two photons both interact on a quark line carrying nearly all of the proton's momentum. This description appears to agree with the Compton data at least at forward angles where $-t < 10$ GeV^2. From this viewpoint, the dominance of the factorizable PQCD leading twist contributions requires momentum transfers much higher than those currently available. However, the endpoint model cannot explain the empirical success of the perturbative QCD fixed $\theta_{c.m.}$ scaling $s^7 d\sigma/dt(\gamma p \to \pi^+ n) \sim$ const at relatively low momentum transfer in pion photoproduction [115].

Clearly much more experimental input on hadron wavefunctions is needed, particularly from measurements of two-photon exclusive reactions into meson and baryon pairs at the high luminosity B factories. For example, the ratio $\frac{d\sigma}{dt}(\gamma\gamma \to \pi^0\pi^0)/\frac{d\sigma}{dt}(\gamma\gamma \to \pi^+\pi^-)$ is particularly sensitive to the shape of pion distribution amplitude. Baryon pair production in two-photon reactions at threshold may reveal physics associated with the soliton structure of baryons in QCD [116, 117]. In addition, fixed target experiments can provide much more information on fundamental QCD processes such as deeply virtual Compton scattering and large angle Compton scattering.

7 Diffractive Dissociation and Light-Cone Wavefunctions

Diffractive dissociation in QCD can be understood as a three-step process:

1. The initial hadron can be decomposed in terms of its quark and gluon constituents in terms of its light-front Fock-state components.

2. In the second step, the incoming hadron is resolved by Pomeron or Odderon (multi-gluon) exchange with the target or by Coulomb dissociation. The exchanged interaction has to supply sufficient momentum transfer q^μ to put the diffracted state X on shell. Light-front energy conservation requires $q^- = (m_X^2 - m_\pi^2)/P_\pi^+$, where m_X is the invariant mass of X. In a heavy target rest system, the longitudinal momentum

transfer is $q^z = (m_X^2 - m_\pi^2)/E_{\pi\mathrm{lab}}$. Thus the momentum transfer $t = q^2$ to the target can be sufficiently small so that the target remains intact.

In perturbative QCD, the pomeron is generally be represented as multiple gluon exchange between the target and projectile. Effectively this interaction occurs over a short light-front time interval, and thus like photon exchange, the perturbative QCD pomeron can be effectively represented as a local operator. This description is believed to be applicable when the pomeron has to resolve compact states and is the basis for the terminology "hard pomeron". The BFKL formalism generalizes the perturbative QCD treatment by an all-orders perturbative resummation, generating a pomeron with a fixed Regge intercept $\alpha_P(0)$. Next to leading order calculations with BLM scale fixing leads to a predicted intercept $\alpha_P(0) \simeq 0.4$ [118]. However, when the exchange interactions are soft, a multiperipheral description in terms of meson ladders may dominate the physics. This is the basis for the two-component pomeron model of Donnachie and Landshoff [119].

Consider a collinear frame where the incident momentum P_π^+ is large and $s = (p_\pi + p_{\mathrm{target}})^2 \simeq p_\pi^+ p_{\mathrm{target}}^-$. The matrix element of an exchanged gluon with momentum q_i between the projectile and an intermediate state $|\,N\rangle$ is dominated by the "plus current": $\left\langle \pi | j^+(0) \exp(i\frac{1}{2} q_i^+ x^- - i q_{\perp i} \cdot x_\perp | N \right\rangle$. Note that the coherent sum of couplings of an exchanged gluon to the pion system vanishes when its momentum is small compared to the characteristic momentum scales in the projectile light-front wavefunction: $q^{\perp_i} \Delta x_\perp \ll 1$ and $q_i^+ \Delta x^- \ll 1$. The destructive interference of the gauge couplings to the constituents of the projectile follows simply from the fact that the color charge operator has zero matrix element between distinct eigenstates of the QCD Hamiltonian: $\langle A|Q|B\rangle \equiv \int d^2x_\perp dx^- \langle A|j^+(0)|B\rangle = 0$ [120]. At high energies the change in k_i^+ of the constituents can be ignored, so that Fock states of a hadron with small transverse size interact weakly even in a nuclear target because of their small dipole moment [30, 27]. To a good approximation the sum of couplings to the constituents of the projectile can be represented as a derivative with respect to transverse momentum. Thus photon exchange measures a weighted sum of transverse derivatives $\partial_{k_\perp} \psi_n(x_i, k_{\perp_i}, \lambda_i)$, and two-gluon exchange measures the second transverse partial derivative [121].

3. The final step is the hadronization of the n constituents of the projectile Fock state into final state hadrons. Since q_i^+ is small, the number of partons in the initial Fock state and the final state hadrons are unchanged. Their coalescence is thus governed by the convolution of initial and final-state Fock state wavefunctions. In the case of states with high $k_\perp$, the final state will hadronize into jets, each reflecting the respective x_i of the Fock state constituents. In the case of higher Fock states with intrinsic sea quarks such as an extra $c\bar{c}$ pair (intrinsic charm), one will observe leading J/ψ or open charm hadrons in the projectile fragmentation region; *i.e.*, the hadron's fragments will tend to have the same rapidity as that of the projectile.

For example, diffractive multi-jet production in heavy nuclei provides a novel way to measure the shape of the LC Fock state wavefunctions and test color transparency. Consider the reaction [27, 28, 122] $\pi A \to \mathrm{Jet}_1 + \mathrm{Jet}_2 + A'$ at high energy where the nucleus A' is left intact in its ground state. The transverse momenta of the jets balance so that $\vec{k}_{\perp i} + \vec{k}_{\perp 2} = \vec{q}_\perp < {R^{-1}}_A$. The light-front longitudinal momentum fractions also need to add to $x_1 + x_2 \sim 1$ so that $\Delta p_L < R_A^{-1}$. The process can then occur coherently in the nucleus. Because of color transparency, the valence wavefunction of the pion with small impact separation, will penetrate the nucleus with minimal interactions, diffracting into jet pairs [27]. The $x_1 = x$, $x_2 = 1 - x$ dependence of the di-jet distributions will thus reflect the shape of the pion valence light-front wavefunction in x; similarly, the $\vec{k}_{\perp 1} - \vec{k}_{\perp 2}$ relative transverse momenta of the jets gives key information on the second derivative of the underlying shape of the valence pion wavefunction [28, 122, 121]. The diffractive nuclear amplitude extrapolated to $t = 0$ should be linear in nuclear number A if color transparency is correct. The integrated diffractive rate should then scale as $A^2/R_A^2 \sim A^{4/3}$.

The results of a diffractive dijet dissociation experiment of this type E791 at Fermilab using 500 GeV incident pions on nuclear targets [123] appear to be consistent with color transparency. The measured longitudinal momentum distribution of the jets [124] is consistent with a pion light-front wavefunction of the pion with the shape of the asymptotic distribution amplitude, $\phi_\pi^{\rm asympt}(x) = \sqrt{3} f_\pi x(1-x)$. Data from CLEO [102] for the $\gamma\gamma^* \to \pi^0$ transition form factor also favor a form for the pion distribution amplitude close to the asymptotic solution to the perturbative QCD evolution equation [5].

The interpretation of the diffractive dijet processes as measures of the hadron distribution amplitudes has recently been questioned by Braun *et al.* [125] and by Chernyak [126] who have calculated the hard scattering amplitude for such processes at next-to-leading order. However, these analyses neglect the integration over the transverse momentum of the valence quarks and thus miss the logarithmic ordering which is required for factorization of the distribution amplitude and color-filtering in nuclear targets.

As noted above, the diffractive dissociation of a hadron or nucleus can also occur via the Coulomb dissociation of a beam particle on an electron beam (*e.g.* at HERA or eRHIC) or on the strong Coulomb field of a heavy nucleus (*e.g.* at RHIC or nuclear collisions at the LHC) [121]. The amplitude for Coulomb exchange at small momentum transfer is proportional to the first derivative $\sum_i e_i \frac{\partial}{k_{Ti}} \psi$ of the light-front wavefunction, summed over the charged constituents. The Coulomb exchange reactions fall off less fast at high transverse momentum compared to pomeron exchange reactions since the light-front wavefunction is effective differentiated twice in two-gluon exchange reactions.

It will also be interesting to study diffractive tri-jet production using proton beams $pA \to \mathrm{Jet}_1 + \mathrm{Jet}_2 + \mathrm{Jet}_3 + A'$ to determine the fundamental shape of the 3-quark structure of the valence light-front wavefunction of the nucleon at small transverse separation [28]. For example, consider the Coulomb dissociation of a high energy proton at HERA. The proton can dissociate into three jets corresponding to the three-quark structure of the valence light-front wavefunction. We can demand that the produced hadrons all fall outside an opening angle θ in the proton's fragmentation region. Effectively all of the light-front momentum $\sum_j x_j \simeq 1$ of the proton's fragments will thus be produced outside an "exclusion cone". This then limits the invariant mass of the contributing Fock state $\mathcal{M}_n^2 > \Lambda^2 = P^{+2} \sin^2 \theta/4$ from below, so that perturbative QCD counting rules can predict the fall-off in the jet system invariant mass $\mathcal{M}$. At large invariant mass one expects the three-quark valence Fock state of the proton to dominate. The segmentation of the forward detector in azimuthal angle ϕ can be used to identify structure and correlations associated with the three-quark light-front wavefunction [121]. An interesting possibility is that the distribution amplitude of the $\Delta(1232)$ for $J_z = 1/2, 3/2$ is close to the asymptotic form $x_1 x_2 x_3$, but that the proton distribution amplitude is more complex. This ansatz can also be motivated by assuming a quark-diquark structure of the baryon wavefunctions. The differences in shapes of the distribution amplitudes could explain why the $p \to \Delta$ transition form factor appears to fall faster at large Q^2 than the elastic $p \to p$ and the other $p \to N^*$ transition form factors [127]. One can use also measure the dijet structure of real and virtual photons beams $\gamma^* A \to \mathrm{Jet}_1 + \mathrm{Jet}_2 + A'$ to measure the shape of the light-front wavefunction for transversely-polarized and longitudinally-polarized virtual photons. Such experiments will open up a direct window on the amplitude structure of hadrons at short distances. The light-front formalism is also applicable to the description of nuclei in terms of their nucleonic and mesonic degrees of freedom [128, 129]. Self-resolving diffractive jet reactions in high energy electron-nucleus collisions and hadron-nucleus collisions at moderate momentum transfers can thus be used to resolve the light-front wavefunctions of nuclei.

The first tests of color transparency involved large momentum transfer quasi-elastic scattering processes in nuclei. Such reactions are predicted in perturbative QCD to depend on the scattering of small impact size hadron wavefunction configurations [30]. The onset of color transparency in proton-proton scattering in nuclei was first seen by Experiment E834 at BNL by observing a rise in the ratio of quasi-elastic to elastic pp scattering at large angles and energies up to $\sqrt{s} \sim 5$ GeV [130]. Quasi-elastic proton-proton scattering is advantageous over the analogous electron-proton scattering reaction since the wavefunctions of the incoming and outgoing hadron in high energy proton reactions would not suffer rapid expansion. However, E834 also revealed another remarkable feature of quasi-elastic pp scattering: the quenching of color transparency at the largest measured energy measured by E834, in direct contradiction to the predictions perturbative QCD. A more recent experiment, E850, using the EVA spectrometer has now confirmed this unexpected effect through new measurements of the transparency ratio at higher energies [32].

The quenching of color transparency observed in the E834 and E850 experiments is almost as important discovery as color transparency itself. It signals a nonperturbative effect in QCD which clearly must be understood. The quenching occurs at the center-of-mass energy of 5 GeV where the pp elastic cross section also displays another remarkable effect: the rate of scattering where the spins of the initial protons are parallel and normal to the scattering plane grows rapidly and becomes approximately 4 times as large as the spin-antiparallel rate [131]. De Teramond and I [132] have noted that both phenomenon occur just at the threshold for open charm hadron production. We have shown in fact that resonance production in pp elastic scattering due to a $uuduudc\bar{c}$ spin-1 resonance will in fact lead to a remarkably large spin correlation A_{NN} and quenching of color transparency above the charm threshold. If this explanation is validated (by the observation of a significant open charm cross section near 5 GeV center of mass energy), then E834 and E850 will have provided the first evidence for an exotic QCD state with hidden charm.

8 Higher Fock States and the Intrinsic Sea

Since a hadronic wavefunction describes states off of the light-front energy shell, there is a finite probability of the projectile having fluctuations containing extra quark-antiquark pairs, such as intrinsic strangeness charm, and bottom. In contrast to the quark pairs arising from gluon splitting, intrinsic quarks are multiply-connected to the valence quarks and are thus part of the dynamics of the hadron.

Recently Franz, Polyakov, and Goeke have analyzed the properties of the intrinsic heavy-quark fluctuations in hadrons using the operator-product expansion [25]. For example, the light-cone momentum fraction carried by intrinsic heavy quarks in the proton $x_{Q\overline{Q}}$ as measured by the T^{++} component of the energy-momentum tensor is related in the heavy-quark limit to the forward matrix element $\langle p|\mathrm{tr}_c(G^{+\alpha}G^{+\beta}G_{\alpha\beta})/m_Q^2|p\rangle$, where $G^{\mu\nu}$ is the gauge field strength tensor. Diagrammatically, this can be described as a heavy quark loop in the proton self-energy with four gluons attached to the light, valence quarks. Since the non-Abelian commutator $[A_\alpha, A_\beta]$ is involved, the heavy quark pairs in the proton wavefunction are necessarily in a color-octet state. It follows from dimensional analysis that the momentum fraction carried by the $Q\overline{Q}$ pair scales as $k_\perp^2/m_Q^2$ where $k_\perp$ is the typical momentum in the hadron wave function. [In contrast, in the case of Abelian theories, the contribution of an intrinsic, heavy lepton pair to the bound state's structure first appears in $O(1/m_L^4)$. One relevant operator corresponds to the Born-Infeld $(F_{\mu\nu})^4$ light-by-light scattering insertion, and the momentum fraction of heavy leptons in an atom scales as $k_\perp^4/m_L^4$.]

The intrinsic sea is thus sensitive to the hadronic bound-state structure [133, 47]. The maximal contribution of an intrinsic heavy quark occurs at $x_Q \simeq m_{\perp Q}/\sum_i m_\perp$ where $m_\perp = \sqrt{m^2 + k_\perp^2}$; *i.e.* at large x_Q, since this minimizes the invariant mass $\mathcal{M}_n^2$. The measurements of the charm structure function by the EMC experiment are consistent with intrinsic charm at large x in the nucleon with a probability of order $0.6 \pm 0.3\%$ [48] which is consistent with the recent estimates based on instanton fluctuations [25].

Thus one can identify two contributions to the heavy quark sea, the "extrinsic" contributions which correspond to ordinary gluon splitting, and the "intrinsic" sea which is multi-connected via gluons to the valence quarks. Intrinsic charm can be materialized by diffractive dissociation into open or hidden charm states such as $pp \to J/\psi X p', \Lambda_c X p'$. At HERA one can measure intrinsic charm in the proton by Coulomb dissociation: $pe \to \Lambda_C X e'$, and $J/\psi X e'$. Since the intrinsic heavy quarks tend to have the same rapidity as that of the projectile, they are produced at large x_F in the beam fragmentation region.

The presence of intrinsic charm quarks in the B wave function provides new mechanisms for B decays. The characteristic momenta characterizing the B meson is most likely higher by a factor of 2 compared to the momentum scale of light mesons, This effect is analogous to the higher momentum scale of muonium $\mu^+ e^-$ versus that of positronium $e^+ e^-$ in atomic physics because of the larger reduced mass. Thus one can expect a higher probability for intrinsic charm in heavy hadrons compared to light hadrons. For example, Chang and Hou have considered the production of final states with three charmed quarks such as $B \to J/\psi D \pi$ and $B \to J/\psi D^*$ [134]; these final states are difficult to realize in the valence model, yet they occur naturally when the b quark of the intrinsic charm Fock state $| b\overline{u} c\overline{c}\rangle$ decays via $b \to c\overline{u}d$. In fact, the J/ψ spectrum for inclusive $B \to J/\psi X$ decays measured by CLEO and Belle shows a distinct enhancement at the low J/ψ momentum where such decays would kinematically occur. Alternatively, this excess could reflect the opening of baryonic channels such as $B \to J/\psi \overline{p} \Lambda$ [135].

Recently, Susan Gardner and I have shown that the presence of intrinsic charm in the hadrons' light-front wave functions, even at a few percent level, provides new, competitive decay mechanisms for B decays which are nominally CKM-suppressed [136]. For example, the weak decays of the B-meson to two-body exclusive states consisting of strange plus light hadrons, such as $B \to \pi K$, are expected to be dominated by penguin contributions since the tree-level $b \to s u \overline{u}$ decay is CKM suppressed. However, higher Fock states in the B wave function containing charm quark pairs can mediate the decay via a CKM-favored $b \to s c \overline{c}$ tree-level transition. Such intrinsic charm contributions can be phenomenologically significant. Since they mimic the amplitude structure of "charming" penguin contributions [137, 138, 139, 140], charming penguins need not be penguins at all [136].

One can also distinguish "intrinsic gluons" [141] which are associated with multi-quark interactions and extrinsic gluon contributions associated with quark substructure. One can also use this framework to isolate the physics of the anomaly contribution to the Ellis-Jaffe sum rule [91]. Thus neither gluons nor sea quarks are solely generated by DGLAP evolution, and one cannot define a resolution scale Q_0 where the sea or gluon degrees of freedom can be neglected.

It is usually assumed that a heavy quarkonium state such as the J/ψ always decays to light hadrons via the annihilation of its heavy quark constituents to gluons. However, as Karliner and I [142] have shown, the transition $J/\psi \to \rho\pi$ can also occur by the rearrangement of the $c\overline{c}$ from the J/ψ into the $|\, q\overline{q}c\overline{c}\rangle$ intrinsic charm Fock state of the ρ or π. On the other hand, the overlap rearrangement integral in the decay $\psi' \to \rho\pi$ will be suppressed since the intrinsic charm Fock state radial wavefunction of the light hadrons will evidently not have nodes in its radial wavefunction. This observation provides a natural explanation of the long-standing puzzle [143] why the J/ψ decays prominently to two-body pseudoscalar-vector final states, breaking hadron helicity conservation [98], whereas the ψ' does not.

The higher Fock state of the proton $|\, uuds\overline{s}\rangle$ should resemble a $|\, K\Lambda\rangle$ intermediate state, since this minimizes its invariant mass $\mathcal{M}$. In such a state, the strange quark has a higher mean momentum fraction x than the $\overline{s}$ [144, 145, 146]. Similarly, the helicity of the intrinsic strange quark in this configuration will be anti-aligned with the helicity of the nucleon [144, 146]. This $Q \leftrightarrow \overline{Q}$ asymmetry is a striking feature of the intrinsic heavy-quark sea.

9 Non-Perturbative Solutions of Light-Front Quantized QCD

Is there any hope of computing light-front wavefunctions from first principles? The solution of the light-front Hamiltonian equation $H_{LC}^{QCD}|\, \Psi\rangle = M^2|\, \Psi\rangle$ is an eigenvalue problem which in principle determines the masses squared of the entire bound and continuum spectrum of QCD. If one introduces periodic or anti-periodic boundary conditions, the eigenvalue problem is reduced to the diagonalization of a discrete Hermitian matrix representation of H_{LC}^{QCD}. The light-front momenta satisfy $x^+ = \frac{2\pi}{L} n_i$ and $P^+ = \frac{2\pi}{L} K$, where $\sum_i n_i = K$. The number of quanta in the contributing Fock states is restricted by the choice of harmonic resolution. A cutoff on the invariant mass of the Fock states truncates the size of the matrix representation in the transverse momenta. This is the essence of the DLCQ method [35], which has now become a standard tool for solving both the spectrum and light-front wavefunctions of one-space one-time theories—virtually any 1+1 quantum field theory, including "reduced QCD" (which has both quark and gluonic degrees of freedom) can be completely solved using DLCQ [147, 73]. The method yields not only the bound-state and continuum spectrum, but also the light-front wavefunction for each eigensolution [148, 149].

Dalley *et al.* have shown how one can use DLCQ in one space-one time, with a transverse lattice to solve mesonic and gluonic states in $3 + 1$ QCD [150]. The spectrum obtained for gluonium states is in remarkable agreement with lattice gauge theory results, but with a huge reduction of numerical effort. Hiller and I [151] have shown how one can use DLCQ to compute the electron magnetic moment in QED without resort to perturbation theory.

There has been recent progress developing the computational tools and renormalization methods which can make DLCQ a viable computational method for QCD in physical space-time. John Hiller, Gary McCartor, and I [11] have shown how DLCQ can be used to solve (3+1) theories and obtain the spectrum and light-front wavefunctions of the bound state solutions despite the large numbers of degrees of freedom needed to enumerate the Fock basis. A key feature of our work is the introduction of Pauli Villars fields [152] in the DLCQ basis which regulate the UV divergences and perform renormalization while preserving the frame-independence of the theory [153, 154].

A recent application of DLCQ and Pauli Villars regularization to a (3+1) quantum field theory with Yukawa interactions is given in Ref. [11]. Only one heavy fermion is allowed in the Fock states. We include an additional effective interaction which represents the contribution of the missing Z graph and cancels an infrared singularity introduced by the instantaneous fermion interaction. Cancellation of ultraviolet infinities is then arranged by choosing imaginary couplings or an indefinite metric. In our most recent work we used three heavy scalars, two of which have negative norm.

In DLCQ, all light-front momentum variables are discretized, with $p^+ \to n\pi/L$ and $\vec{p}_\perp \to \vec{n}_\perp \pi/L_\perp$, in terms of longitudinal and transverse length scales L and $L_\perp$. The total longitudinal momentum is $P^+ = K\pi/L$ and momentum fractions are given by $x = n/K$. Wave functions and the mass eigenvalue problem, where $H_{\rm LC} = P^+P^-$, are naturally expressed in terms of momentum fractions and the resolution K. Hence L disappears, and K effectively takes its place as the resolution scale. The transverse scale $L_\perp$ is set by a momentum cutoff and a transverse resolution. The integrals over wave functions which make up the mass eigenvalue problem $H_{\rm LC}\Phi = M^2\Phi$ are then approximated by the trapezoidal quadrature rule. This yields a matrix eigenvalue problem which is typically quite large but also quite sparse. Lanczos techniques [155] are used to extract eigenvalues and eigenvectors for the lowest states, even in the case of an indefinite metric [11].

The mass M of the dressed single-fermion state is held fixed. This is imposed by rearranging the mass eigenvalue problem into an eigenvalue problem for the quantity δM^2:

$$\begin{aligned} x\left[M^2 - \frac{M^2+p_\perp^2}{x} - \sum_j \frac{\mu_j^2+q_{\perp j}^2}{y_j}\right]\tilde{\phi} \\ -\int \prod_j dy_j' d^2 q_{\perp j}' \sqrt{xx'}\mathcal{K}\tilde{\phi}' = \delta M^2 \tilde{\phi}\,, \end{aligned} \tag{37}$$

where $\mathcal{K}$ represents the original kernel and amplitudes are related by $\phi = \sqrt{x}\tilde{\phi}$.

The coupling g is constrained by imposing a condition on the boson occupation number: $\langle{:}\phi^2(0){:}\rangle \equiv \Phi_\sigma^\dagger {:}\phi^2(0){:} \Phi_\sigma$. This quantity can be computed fairly efficiently as

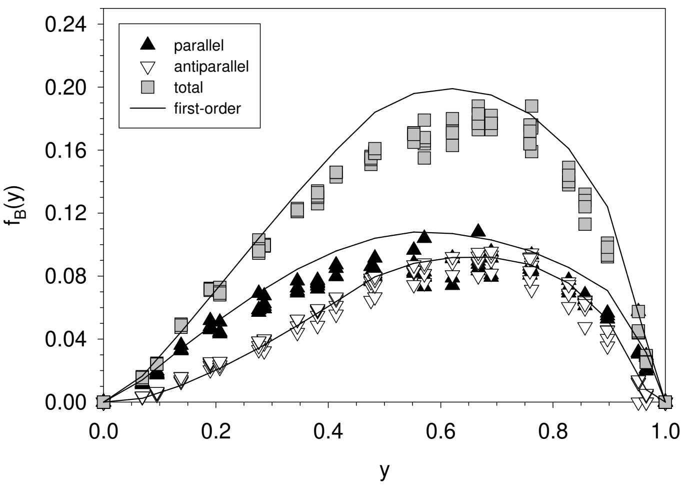

Figure 7: The boson structure function f_B at various numerical resolutions for $\langle{:}\phi^2(0){:}\rangle = 0.5$, with $M = \mu$, cutoff $\Lambda^2 = 50\mu^2$, and Pauli–Villars masses $\mu_1^2 = 10\mu^2$, $\mu_2^2 = 20\mu^2$, and $\mu_3^2 = 30\mu^2$. The solid line is from first-order perturbation theory.

the sum

$$\langle{:}\phi^2(0){:}\rangle = \sum_{n_i=0}^{\infty} \int \prod_j^{n_{\rm tot}} dq_j^+ d^2q_{\perp j} \sum_s (-1)^{(n_i)} \times \left(\sum_{k=1}^{n} \frac{2}{q_k^+/P^+}\right) \left|\phi_{\sigma s}^{(n_i)}(\underline{q}_j; \underline{P} - \sum_j \underline{q}_j)\right|^2 . \tag{38}$$

The constraint on $\langle{:}\phi^2(0){:}\rangle$ can be satisfied by solving it simultaneously with the eigenvalue problem.

With the parameters fixed, we can compute various quantities, such as the parton wavefunctions and momentum distributions, the form factor slope at zero momentum transfer, the average numbers of constituents, and the average constituent momenta. A representative plot of the bosonic structure function

$$f_B(y) \equiv \sum_{n_i=0}^{\infty} \sum_s \int \prod_j dq_j^+ d^2q_{\perp j} (-1)^{(n_i)} \sum_{k=1}^{n_0} \times \delta(y - q_k^+/P^+) \left|\phi_{\sigma s}^{(n_i)}(\underline{q}_j; \underline{P} - \sum_i \underline{q}_j)\right|^2 , \tag{39}$$

is given in Fig. 7. We have also worked at somewhat stronger couplings where deviations from first order perturbation theory becomes apparent; however, high resolution is required, with $K = 21$ to 39 and as many as 15 transverse momentum points. This resolution could be achieved by limiting the number of constituents to 3, after verifying that the contribution from higher sectors was sufficiently small.

The success of application of DLCQ to the Yukawa theory with Pauli-Villars regularization is encouraging. One can compute masses and wave functions for eigenstates for quantum field theories in physical space-time. Another procedure, now under investigation, is to use one heavy scalar and one heavy fermion, both with negative norm, as suggested by the work of Paston *et al.* [156] This method has the advantage of being free of instantaneous fermion interactions. An alternative and interesting regularization is to apply DLCQ to finite supersymmetric 3+1 theories, and then introduce supersymmetric breaking.

We plan to continue to be explored these possibilities with various model theories, leading eventually to the direct application to QCD(3+1). In fact, Paston *et al.* [157] have already obtained a PV-like regularization of QCD which could, in principle, be solved by DLCQ; however, given present computing power the number of fields is possibly too large for meaningful calculations.

One can also formulate DLCQ so that supersymmetry is exactly preserved in the discrete approximation, thus combining the power of DLCQ with the beauty of supersymmetry [158, 159, 160]. The "SDLCQ" method has been applied to several interesting supersymmetric theories, to the analysis of zero modes, vacuum degeneracy, massless states, mass gaps, and theories in higher dimensions, and even tests of the Maldacena conjecture [158]. Broken supersymmetry is interesting in DLCQ, since it may serve as a method for regulating non-Abelian theories [154].

There are also many possibilities for obtaining approximate solutions of light-front wavefunctions in QCD. QCD sum rules, lattice gauge theory moments, and QCD inspired models such as the bag model, chiral theories, provide important constraints. Guides to the exact behavior of LC wavefunctions in QCD can also be obtained from analytic or DLCQ solutions to toy models such as "reduced" $QCD(1+1)$. The light-front and many-body Schrödinger theory formalisms must match In the nonrelativistic limit.

It would be interesting to see if light-front wavefunctions can incorporate chiral constraints such as soliton (Skyrmion) behavior for baryons and other consequences of the chiral limit in the soft momentum regime. Solvable theories such as $QCD(1+1)$ are also useful for understanding such phenomena. It has been shown that the anomaly contribution for the $\pi^0 \to \gamma\gamma$ decay amplitude is satisfied by the light-front Fock formalism in the limit where the mass of the pion is light compared to its size [161].

10 Non-Perturbative Calculations of the Pion Distribution Amplitude

The distribution amplitude $\phi(x, \widetilde{Q})$ can be computed from the integral over transverse momenta of the renormalized hadron valence wavefunction in the light-cone gauge at fixed light-front time [38]:

$$\phi(x, \widetilde{Q}) = \int d^2\vec{k_\perp}\, \theta\left(\widetilde{Q}^2 - \frac{\vec{k_\perp}^{\,2}}{x(1-x)}\right) \psi^{(\widetilde{Q})}(x, \vec{k_\perp}), \tag{40}$$

where a global cutoff in invariant mass is identified with the resolution $\tilde{Q}$. The distribution amplitude $\phi(x, \tilde{Q})$ is boost and gauge invariant and evolves in $\ln \tilde{Q}$ through an evolution equation [93, 90, 5]. Since it is formed from the same product of operators as the non-singlet structure function, the anomalous dimensions controlling $\phi(x, Q)$ dependence in the ultraviolet $\log Q$ scale are the same as those which appear in the DGLAP evolution of structure functions [55]. The decay $\pi \to \mu\nu$ normalizes the wave function at the origin: $a_0/6 = \int_0^1 dx \phi(x, Q) = f_\pi/(2\sqrt{3})$. One can also compute the distribution amplitude from the gauge invariant Bethe-Salpeter wavefunction at equal light-front time. This also allows contact with both QCD sum rules and lattice gauge theory; for example, moments of the pion distribution amplitudes have been computed in lattice gauge theory [162, 163, 164].

Dalley [107] has recently calculated the pion distribution amplitude from QCD using a combination of the discretized DLCQ method for the x^- and x^+ light-front coordinates with the transverse lattice method [165, 166] in the transverse directions, A finite lattice spacing a can be used by choosing the parameters of the effective theory in a region of renormalization group stability to respect the required gauge, Poincaré, chiral, and continuum symmetries. The overall normalization gives $f_\pi = 101$ MeV compared with the experimental value of 93 MeV. Figure 5 (a) compares the resulting DLCQ/transverse lattice pion wavefunction with the best fit to the diffractive di-jet data (see the next section) after corrections for hadronization and experimental acceptance [26]. The theoretical curve is somewhat broader than the experimental result. However, there are experimental uncertainties from hadronization and theoretical errors introduced from finite DLCQ resolution, using a nearly massless pion, ambiguities in setting the factorization scale Q^2, as well as errors in the evolution of the distribution amplitude from 1 to 10 GeV^2. Instanton models also predict a pion distribution amplitude close to the asymptotic form [167]. In contrast, recent lattice results from Del Debbio *et al.* [164] predict a much narrower shape for the pion distribution amplitude than the distribution predicted by the transverse lattice. A new result for the proton distribution amplitude treating nucleons as chiral solitons has recently been derived by Diakonov and Petrov [168]. Dyson-Schwinger models [169] of hadronic Bethe-Salpeter wavefunctions can also be used to predict light-front wavefunctions and hadron distribution amplitudes by integrating over the relative k^- momentum. There is also the possibility of deriving Bethe-Salpeter wavefunctions within light-front gauge quantized QCD [41] in order to properly match to the light-cone gauge Fock state decomposition.

11 Calculating and Modelling Light-Front Wavefunctions

Many features of the light-front wavefunctions follow from general arguments. Light-front wavefunctions satisfy the equation of motion:

$$H_{LC}^{QCD}|\,\Psi\rangle = (H_{LC}^0 + V_{LC})|\,\Psi\rangle = M^2|\,\Psi\rangle,$$

which has the Heisenberg matrix form in Fock space:

$$[M^2 - \sum_{i=1}^{n} \frac{m_{\perp i}^2}{x_i}]\psi_n = \sum_{n'} \int \langle n|V|n'\rangle\, \psi_{n'}$$

where the convolution and sum is understood over the Fock number, transverse momenta, plus momenta and helicity of the intermediate states. Here $m_\perp^2 = m^2 + k_\perp^2$. Thus, in general, every light-front Fock wavefunction has the form:

$$\psi_n = \frac{\Gamma_n}{M^2 - \sum_{i=1}^n \frac{m_{\perp i}^2}{x_i}}$$

where $\Gamma_n = \sum_{n'} \int V_{nn'}\psi_n$. The main dynamical dependence of a light-front wavefunction away from the extrema is controlled by its light-front energy denominator. The maximum of the wavefunction occurs when the invariant mass of the partons is minimal; *i.e.*, when all particles have equal rapidity and are all at rest in the rest frame. In fact, Dae Sung Hwang and I [120] have noted that one can rewrite the wavefunction in the form:

$$\psi_n = \frac{\Gamma_n}{M^2[\sum_{i=1}^n \frac{(x_i - \hat{x}_i)^2}{x_i} + \delta^2]}$$

where $x_i = \hat{x}_i \equiv m_{\perp i}/\sum_{i=1}^n m_{\perp i}$ is the condition for minimal rapidity differences of the constituents. The key parameter is $M^2 - \sum_{i=1}^n m_{\perp i}^2/\hat{x}_i \equiv -M^2\delta^2$. We can also interpret $\delta^2 \simeq 2\epsilon/M$ where $\epsilon = \sum_{i=1}^n m_{\perp i} - M$ is the effective binding energy. This form shows that the wavefunction is a quadratic form around its maximum, and that the width of the distribution in $(x_i - \hat{x}_i)^2$ (where the wavefunction falls to half of its maximum) is controlled by $x_i\delta^2$ and the transverse momenta $k_{\perp_i}$. Note also that the heaviest particles tend to have the largest $\hat{x}_i$, and thus the largest momentum fraction of the particles in the Fock state, a feature familiar from the intrinsic charm model. For example, the b quark has the largest momentum fraction at small $k_\perp$ in the B meson's valence light-front wavefunction,, but the distribution spreads out to an asymptotically symmetric distribution around $x_b \sim 1/2$ when $k_\perp \gg m_b^2$.

We can also discern some general properties of the numerator of the light-front wavefunctions. $\Gamma_n(x_i, k_{\perp i}, \lambda_i)$. The transverse momentum dependence of Γ_n guarantees J_z conservation for each Fock state. For example, one of the three light-front Fock wavefunctions of a $J_z = +1/2$ lepton in QED perturbation theory is $\psi^{\uparrow}_{+\frac{1}{2}+1}(x, \vec{k}_\perp) = -\sqrt{2}\frac{(-k^1+{\rm i}k^2)}{x(1-x)}\,\varphi$, where $\varphi = \varphi(x, \vec{k}_\perp) = \frac{e/\sqrt{1-x}}{M^2-(\vec{k}_\perp^2+m^2)/x-(\vec{k}_\perp^2+\lambda^2)/(1-x)}$. The orbital angular momentum projection in this case is $\ell^z = -1$. The spin structure indicated by perturbative theory provides a template for the numerator structure of the light-front wavefunctions even for composite systems. The structure of the electron's Fock state in perturbative QED shows that it is natural to have a negative contribution from relative orbital angular momentum which balances the S_z of its photon constituents. We can also expect a significant orbital contribution to the proton's J_z since gluons carry roughly half of the proton's momentum, thus providing insight into the "spin crisis" in QCD.

The high $x \to 1$ and high $k_\perp$ limits of the hadron wavefunctions control processes and reactions in which the hadron wavefunctions are highly stressed. Such configurations involve far-off-shell intermediate states and can be systematically treated in perturbation theory [170, 5]. This leads to counting rule behavior for the quark and gluon distributions at $x \to 1$. Notice that $x \to 1$ corresponds to $k^z \to -\infty$ for any constituent with nonzero mass or transverse momentum.

The above discussion suggests that an approximate form for the hadron light-front wavefunctions could be constructed through variational principles and by minimizing the expectation value of H^{QCD}_{LC}.

12 Structure Functions are Not Parton Distributions

Ever since the earliest days of the parton model, it has been assumed that the leading-twist structure functions $F_i(x, Q^2)$ measured in deep inelastic lepton scattering are determined by the *probability* distribution of quarks and gluons as determined by the light-front wavefunctions of the target. For example, the quark distribution is

$$P_{{\rm q}/N}(x_B, Q^2) = \sum_n \int^{k_{i\perp}^2<Q^2} \left[\prod_i dx_i\, d^2k_{\perp i}\right] |\psi_n(x_i, k_{\perp i})|^2 \sum_{j=q} \delta(x_B - x_j).$$

The identification of structure functions with the square of light-front wavefunctions is usually made in LC gauge $n \cdot A = A^+ = 0$, where the path-ordered exponential in

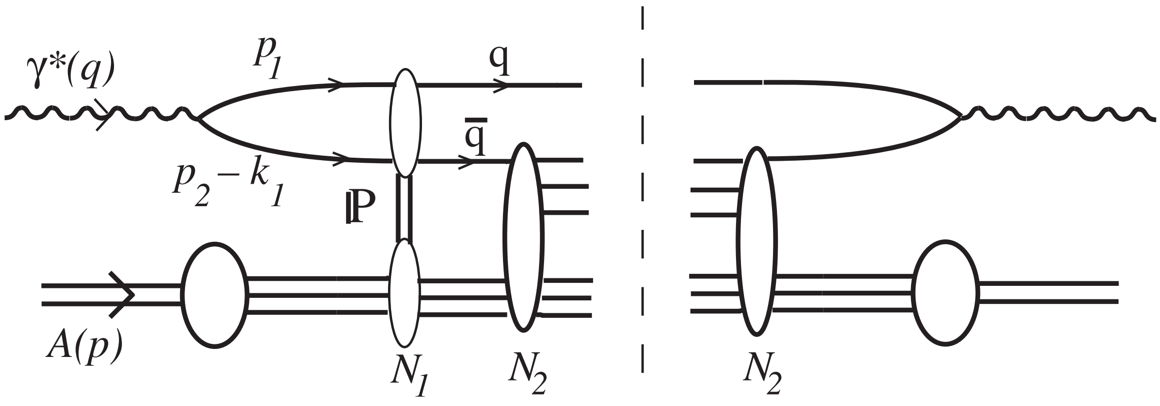

Figure 8: Glauber-Gribov shadowing involves interference between rescattering amplitudes.

the operator product for the forward virtual Compton amplitude apparently reduces to unity. Thus the deep inelastic lepton scattering cross section (DIS) appears to be fully determined by the probability distribution of partons in the target. However, Paul Hoyer, Nils Marchal, Stephane Peigne, Francesco Sannino, and I [171] have recently shown that the leading-twist contribution to DIS is affected by diffractive rescattering of a quark in the target, a coherent effect which is not included in the light-front wavefunctions, even in light-cone gauge. The distinction between structure functions and parton probabilities is already implied by the Glauber-Gribov picture of nuclear shadowing [172, 173, 174, 175]. In this framework shadowing arises from interference between complex rescattering amplitudes involving on-shell intermediate states, as in Fig. 8. In contrast, the wave function of a stable target is strictly real since it does not have on energy-shell configurations. A probabilistic interpretation of the DIS cross section is thus precluded.

It is well-known that in Feynman and other covariant gauges one has to evaluate the corrections to the "handbag" diagram due to the final state interactions of the struck quark (the line carrying momentum p_1 in Fig. 9) with the gauge field of the target. In light-cone gauge, this effect also involves rescattering of a spectator quark, the p_2 line in Fig. 9. The light-cone gauge is singular – in particular, the gluon propagator $d^{\mu\nu}_{LC}(k) = \frac{i}{k^2+i\varepsilon}\left[-g^{\mu\nu} + \frac{n^\mu k^\nu + k^\mu n^\nu}{n\cdot k}\right]$ has a pole at $k^+ = 0$ which requires an analytic prescription. In final-state scattering involving on-shell intermediate states, the exchanged momentum k^+ is of $O\left(1/\nu\right)$ in the target rest frame, which enhances the second term in the propagator. This enhancement allows rescattering to contribute at leading twist even in LC gauge.

The issues involving final state interactions even occur in the simple framework of abelian gauge theory with scalar quarks. Consider a frame with $q^+ < 0$. We can then distinguish FSI from ISI using LC time-ordered perturbation theory [5].

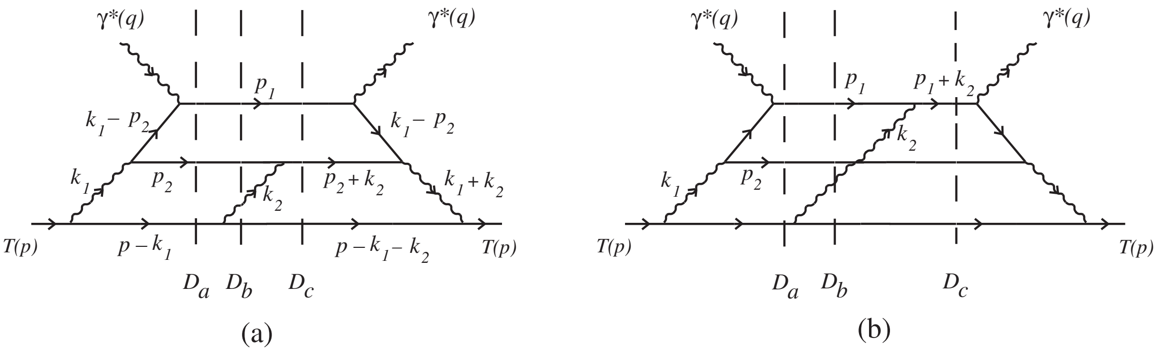

Figure 9: Two types of final state interactions. (a) Scattering of the antiquark (p_2 line), which in the aligned jet kinematics is part of the target dynamics. (b) Scattering of the current quark (p_1 line). For each LC time-ordered diagram, the potentially on-shell intermediate states – corresponding to the zeroes of the denominators D_a, D_b, D_c – are denoted by dashed lines.

Figure 9 illustrates two LCPTH diagrams which contribute to the forward $\gamma^* T \to \gamma^* T$ amplitude, where the target T is taken to be a single quark. In the aligned jet kinematics the virtual photon fluctuates into a $q\overline{q}$ pair with limited transverse momentum, and the (struck) quark takes nearly all the longitudinal momentum of the photon. The initial q and $\overline{q}$ momenta are denoted p_1 and $p_2 - k_1$, respectively,

The calculation of the rescattering effect of DIS in Feynman and light-cone gauge through three loops is given in detail in Ref. [171]. The result can be resummed and is most easily expressed in eikonal form in terms of transverse distances $r_\perp, R_\perp$ conjugate to $p_{2\perp}, k_\perp$. The deep inelastic cross section can be expressed as

$$Q^4 \frac{d\sigma}{dQ^2\, dx_B} = \frac{\alpha}{16\pi^2} \frac{1-y}{y^2} \frac{1}{2M\nu} \int \frac{dp_2^-}{p_2^-} \, d^2\vec{r}_\perp \, d^2\vec{R}_\perp \, |\tilde{M}|^2 \tag{41}$$

where

$$|\tilde{M}(p_2^-, \vec{r}_\perp, \vec{R}_\perp)| = \left| \frac{\sin\left[g^2 \, W(\vec{r}_\perp, \vec{R}_\perp)/2\right]}{g^2 \, W(\vec{r}_\perp, \vec{R}_\perp)/2} \tilde{A}(p_2^-, \vec{r}_\perp, \vec{R}_\perp) \right| \tag{42}$$

is the resummed result. The Born amplitude is

$$\tilde{A}(p_2^-, \vec{r}_\perp, \vec{R}_\perp) = 2eg^2 MQp_2^- \, V(m_{||} r_\perp) W(\vec{r}_\perp, \vec{R}_\perp) \tag{43}$$

where $m_{||}^2 = p_2^- M x_B + m^2$ and

$$V(m\, r_\perp) \equiv \int \frac{d^2\vec{p}_\perp}{(2\pi)^2} \frac{e^{i\vec{r}_\perp \cdot \vec{p}_\perp}}{p_\perp^2 + m^2} = \frac{1}{2\pi} K_0(m\, r_\perp) \tag{44}$$

The rescattering effect of the dipole of the $q\overline{q}$ is controlled by

$$W(\vec{r}_\perp, \vec{R}_\perp) \equiv \int \frac{d^2\vec{k}_\perp}{(2\pi)^2} \frac{1 - e^{i\vec{r}_\perp \cdot \vec{k}_\perp}}{k_\perp^2} e^{i\vec{R}_\perp \cdot \vec{k}_\perp} = \frac{1}{2\pi} \log \left(\frac{|\vec{R}_\perp + \vec{r}_\perp|}{R_\perp} \right). \tag{45}$$

The fact that the coefficient of $\tilde{A}$ in (42) is less than unity for all $\vec{r}_\perp, \vec{R}_\perp$ shows that the rescattering corrections reduce the cross section. It is the analog of nuclear shadowing in our model.

We have also found the same result for the deep inelastic cross sections in light-cone gauge. Three prescriptions for defining the propagator pole at $k^+ = 0$ have been used in the literature:

$$\frac{1}{k_i^+} \rightarrow \left[\frac{1}{k_i^+}\right]_{\eta_i} = \begin{cases} k_i^+ \left[(k_i^+ - i\eta_i)(k_i^+ + i\eta_i)\right]^{-1} & \text{(PV)} \\ \left[k_i^+ - i\eta_i\right]^{-1} & \text{(K)} \\ \left[k_i^+ - i\eta_i \epsilon(k_i^-)\right]^{-1} & \text{(ML)} \end{cases} \tag{46}$$

the principal-value, Kovchegov [176], and Mandelstam-Leibbrandt [177] prescriptions. The 'sign function' is denoted $\epsilon(x) = \Theta(x) - \Theta(-x)$. With the PV prescription we have $I_\eta = \int dk_2^+ \left[\frac{1}{k_2^+}\right]_{\eta_2} = 0$. Since an individual diagram may contain pole terms $\sim 1/k_i^+$, its value can depend on the prescription used for light-cone gauge. However, the $k_i^+ = 0$ poles cancel when all diagrams are added; the net is thus prescription-independent, and it agrees with the Feynman gauge result. It is interesting to note that the diagrams involving rescattering of the struck quark p_1 do not contribute to the leading-twist structure functions if we use the Kovchegov prescription to define the light-cone gauge. In other prescriptions for light-cone gauge the rescattering of the struck quark line p_1 leads to an infrared divergent phase factor $\exp i\phi$:

$$\phi = g^2 \, \frac{I_\eta - 1}{4\pi} \, K_0(\lambda R_\perp) + O(g^6) \tag{47}$$

where λ is an infrared regulator, and $I_\eta = 1$ in the K prescription. The phase is exactly compensated by an equal and opposite phase from final-state interactions of line p_2. This irrelevant change of phase can be understood by the fact that the different prescriptions are related by a residual gauge transformation proportional to $\delta(k^+)$ which leaves the light-cone gauge $A^+ = 0$ condition unaffected.

Diffractive contributions which leave the target intact thus contribute at leading twist to deep inelastic scattering. These contributions do not resolve the quark structure of the target, and thus they are contributions to structure functions which are not parton probabilities. More generally, the rescattering contributions shadow and modify the observed inelastic contributions to DIS.

Our analysis in the K prescription for light-cone gauge resembles the "covariant parton model" of Landshoff, Polkinghorne and Short [178, 76] when interpreted in the target rest frame. In this description of small x DIS, the virtual photon with positive q^+ first splits into the pair p_1 and p_2. The aligned quark p_1 has no final state interactions. However, the antiquark line p_2 can interact in the target with an effective energy $\hat{s} \propto k_\perp^2/x$ while staying close to its mass shell. Thus at small x and large $\hat{s}$, the antiquark p_2 line can first multiple scatter in the target via pomeron and Reggeon exchange, and then it can finally scatter inelastically or be annihilated. The DIS cross section can thus be written as an integral of the $\sigma_{\overline{q}p\to X}$ cross section over the p_2 virtuality. In this way, the shadowing of the antiquark in the nucleus $\sigma_{\overline{q}A\to X}$ cross section yields the nuclear shadowing of DIS [174]. Our analysis, when interpreted in frames with $q^+ > 0$, also supports the color dipole description of deep inelastic lepton scattering at small x. Even in the case of the aligned jet configurations, one can understand DIS as due to the coherent color gauge interactions of the incoming quark-pair state of the photon interacting first coherently and finally incoherently in the target.

13 A Light-Front Event Amplitude Generator

The light-front formalism can be used as an "event amplitude generator" for high energy physics reactions where each particle's final state is completely labelled in momentum, helicity, and phase. The application of the light-front time evolution operator P^- to an initial state systematically generates the tree and virtual loop graphs of the T-matrix in light-front time-ordered perturbation theory in light-cone gauge. The loop integrals only involve integrations over the momenta of physical quanta and physical phase space $\prod d^2k_{\perp i}dk_i^+$. Renormalized amplitudes can be explicitly constructed by subtracting from the divergent loops amplitudes with nearly identical integrands corresponding to the contribution of the relevant mass and coupling counter terms (the "alternating denominator method") [4]. The natural renormalization scheme to use for defining the coupling in the event amplitude generator is a physical effective charge such as the pinch scheme [39]. The argument of the coupling is then unambiguous [179]. The DLCQ boundary conditions can be used to discretize the phase space and limit the number of contributing intermediate states without violating Lorentz invariance. Since one avoids dimensional regularization and nonphysical ghost degrees of freedom, this method of generating events at the amplitude level could provide a simple but powerful tool for simulating events both in QCD and the Standard Model.

14 The Light-Front Partition Function

In the usual treatment of classical thermodynamics, one considers an ensemble of particles $n = 1, 2, ...N$ which have energies $\{E_n\}$ at a given "instant" time t. The partition function is defined as $Z = \sum_n \exp -\frac{E_n}{kT}$. Similarly, in quantum mechanics, one defines a quantum-statistical partition function as $Z = tr \exp -\beta H$ which sums over the exponentiated-weighted energy eigenvalues of the system.

In the case of relativistic systems, it is natural to characterize the system at a given light-front time $\tau = t + z/c$; i.e., one determines the state of each particle in the ensemble as its encounters the light-front. Thus we can define a light-front partition function

$$Z_{LC} = \sum_n \exp -\frac{p_n^-}{kT_{LC}}$$

by summing over the particles' light-front energies $p^- = p^0 - p^z = \frac{p_\perp^2 + m^2}{p^+}$. The total momentum is $P^+ = \sum p_n^+$, $\vec{P}_\perp = \sum_n \vec{p}_{\perp n}$, and the total mass is defined from $P^+ P^- - P_\perp^2 = M^2$. The product $\frac{M}{P^-} T_{LC}$ is boost invariant. In the center of mass frame where $\vec{P} = 0$ and thus $P^+ = P^- = M$. It is also possible to consistently impose boundary conditions at fixed $x^- = z - ct$ and $x_\perp$, as in DLCQ. The momenta $p_n^+, \vec{p}_{\perp n}$ then become discrete. The corresponding light-front quantum-statistical partition function is $Z = tr \exp -\beta_{LC} H_{LC}$ where $H_{LC} = i\frac{\partial}{\partial\tau}$ is the light-front Hamiltonian.

For non-relativistic systems the light-front partition function reduces to the standard definition. However, the light-front partition function should be advantageous for analyzing relativistic systems such as heavy ion collisions, since, like true rapidity, $y = \ln \frac{p^+}{P^+}$, light-front variables have simple behavior under Lorentz boosts. The light-front formalism also takes into account the point that a phase transition does not occur simultaneously in t, but propagates through the system with a finite wave velocity.

Acknowledgments

Work supported by the Department of Energy under contract number DE-AC03-76SF00515. I wish to thank the organizers of this meeting, A. Bialas, M. A. Nowak, and M. Sadzikowski for their outstanding hospitality in Zakopane. Much of this work is based on collaborations, particularly with Markus Diehl, Paul Hoyer, Dae Sung Hwang, Peter Lepage, Bo-Qiang Ma, Hans Christian Pauli Ivan Schmidt, and Prem Srivastava.

References

[1] P. A. Dirac, Rev. Mod. Phys. **21**, 392 (1949).

[2] For a review and references, see S. J. Brodsky, H. C. Pauli and S. S. Pinsky, Phys. Rept. **301**, 299 (1998) [arXiv:hep-ph/9705477].

[3] S. Weinberg, Phys. Rev. **150**, 1313 (1966).

[4] S. J. Brodsky, R. Roskies and R. Suaya, Momentum Frame," Phys. Rev. D **8**, 4574 (1973).

[5] G. P. Lepage and S. J. Brodsky, Phys. Rev. D **22**, 2157 (1980).

[6] T. Maskawa and K. Yamawaki, Method Of Quantization," Prog. Theor. Phys. **56**, 270 (1976).

[7] H. C. Pauli and S. J. Brodsky, Phys. Rev. D **32**, 1993 (1985).

[8] A. Abada, P. Boucaud, G. Herdoiza, J. P. Leroy, J. Micheli, O. Pene and J. Rodriguez-Quintero, Phys. Rev. D **64**, 074511 (2001) [arXiv:hep-ph/0105221].

[9] Y. Matsumura, N. Sakai and T. Sakai, Phys. Rev. D **52**, 2446 (1995) [arXiv:hep-th/9504150].

[10] J. R. Hiller, S. Pinsky and U. Trittmann, supersymmetric Yang-Mills theory," Phys. Rev. D **64**, 105027 (2001) [arXiv:hep-th/0106193].

[11] S. J. Brodsky, J. R. Hiller and G. McCartor, hep-ph/0107038.

[12] W. A. Bardeen, R. B. Pearson and E. Rabinovici, Phys. Rev. D **21**, 1037 (1980).

[13] S. Dalley, Phys. Rev. D **64**, 036006 (2001) [arXiv:hep-ph/0101318].

[14] M. Burkardt and S. K. Seal, arXiv:hep-ph/0105109.

[15] H. C. Pauli, arXiv:hep-ph/0111040.

[16] G. McCartor, in Proc. of New Nonperturbative Methods and Quantization of the Light Cone, Les Houches, France, 24 Feb - 7 Mar 1997.

[17] K. Yamawaki, arXiv:hep-th/9802037.

[18] S. J. Brodsky, D. S. Hwang, B. Q. Ma and I. Schmidt, Nucl. Phys. B **593**, 311 (2001) [arXiv:hep-th/0003082].

[19] S. D. Drell and T. Yan, Phys. Rev. Lett. **24**, 181 (1970).

[20] G. B. West, Phys. Rev. Lett. **24**, 1206 (1970).

[21] S. J. Brodsky and S. D. Drell, Phys. Rev. D **22**, 2236 (1980).

[22] S. J. Brodsky and D. S. Hwang, Nucl. Phys. B **543**, 239 (1999) [hep-ph/9806358].

[23] S. J. Brodsky, M. Diehl and D. S. Hwang, hep-ph/0009254.

[24] M. Diehl, T. Feldmann, R. Jakob and P. Kroll, hep-ph/0009255.

[25]

[25] M. Franz, M. V. Polyakov and K. Goeke, Phys. Rev. D **62**, 074024 (2000) [hep-ph/0002240].

[26] D. Ashery [E791 Collaboration], hep-ex/9910024.

[27] G. Bertsch, S. J. Brodsky, A. S. Goldhaber and J. F. Gunion, Phys. Rev. Lett. **47**, 297 (1981).

[28] L. Frankfurt, G. A. Miller and M. Strikman, Phys. Lett. **B304**, 1 (1993) [hep-ph/9305228].

[29] L. Frankfurt, G. A. Miller and M. Strikman, Found. Phys. **30**, 533 (2000) [hep-ph/9907214].

[30] S. J. Brodsky and A. H. Mueller, Phys. Lett. **B206**, 685 (1988).

[31] L. L. Frankfurt and M. I. Strikman, Phys. Rept. **160**, 235 (1988).

[32] A. Leksanov *et al.*, Phys. Rev. Lett. **87**, 212301 (2001) [arXiv:hep-ex/0104039].

[33] M. Beneke, G. Buchalla, M. Neubert and C. T. Sachrajda, Phys. Rev. Lett. **83**, 1914 (1999) [hep-ph/9905312].

[34] Y. Keum, H. Li and A. I. Sanda, hep-ph/0004004.

[35] H. C. Pauli and S. J. Brodsky, Phys. Rev. D **32**, 2001 (1985).

[36] S. J. Brodsky, H. Pauli and S. S. Pinsky, Phys. Rept. **301**, 299 (1998) [hep-ph/9705477].

[37] P. P. Srivastava and S. J. Brodsky, Phys. Rev. D **64**, 045006 (2001) [arXiv:hep-ph/0011372].

[38] S. J. Brodsky and G. P. Lepage, in *Perturbative Quantum Chromodynamics*, A. H. Mueller, Ed. (World Scientific, 1989).

[39] J. M. Cornwall and J. Papavassiliou, Phys. Rev. D **40**, 3474 (1989).

[40] S. J. Brodsky, E. Gardi, G. Grunberg and J. Rathsman, hep-ph/0002065.

[41] P. P. Srivastava and S. J. Brodsky, Phys. Rev. **D61**, 025013 (2000), hep-ph/9906423, and SLAC-PUB 8543, in preparation.

[42] A. Bassetto, L. Griguolo and F. Vian, hep-th/9911036.

[43] G. McCartor, hep-th/0004139.

[44] P. P. Srivastava, Phys. Lett. **B448**, 68 (1999) [hep-th/9811225].

[45] S. S. Pinsky and B. van de Sande, Phys. Rev. **D49**, 2001 (1994), hep-ph/9310330.

[46] S. J. Brodsky, hep-ph/0006310.

[47] S. J. Brodsky, P. Hoyer, C. Peterson and N. Sakai, Phys. Lett. **B93**, 451 (1980).

[48] B. W. Harris, J. Smith and R. Vogt, Nucl. Phys. **B461**, 181 (1996) [hep-ph/9508403].

[49] F. Antonuccio, S. J. Brodsky and S. Dalley, Phys. Lett. **B412**, 104 (1997) [hep-ph/9705413].

[50] S. J. Brodsky and B. T. Chertok, Phys. Rev. D **14**, 3003 (1976).

[51] S. J. Brodsky, C. Ji and G. P. Lepage, Phys. Rev. Lett. **51**, 83 (1983).

[52] G. R. Farrar, K. Huleihel and H. Zhang, Phys. Rev. Lett. **74**, 650 (1995).

[53] S. J. Brodsky, E. Chudakov, P. Hoyer and J. M. Laget, hep-ph/0010343.

[54] S. J. Brodsky and J. Rathsman, hep-ph/9906339.

[55] S. J. Brodsky, Y. Frishman, G. P. Lepage and C. Sachrajda, *Phys. Lett.* **91B**, 239 (1980).

[56] D. Müller, *Phys. Rev.* **D49**, 2525 (1994).

[57] V. M. Braun, S. E. Derkachov, G. P. Korchemsky and A. N. Manashov, Nucl. Phys. **B553**, 355 (1999), hep-ph/9902375.

[58] S. J. Brodsky and H. J. Lu, *Phys. Rev.* **D51**, 3652 (1995), hep-ph/9405218.

[59] S. J. Brodsky, J. R. Pelaez and N. Toumbas, Phys. Rev. **D60**, 037501 (1999), hep-ph/9810424.

[60] S. J. Brodsky, G. T. Gabadadze, A. L. Kataev and H. J. Lu, *Phys. Lett.* **B372**, 133 (1996) hep-ph/9512367.

[61] S. J. Brodsky, M. S. Gill, M. Melles and J. Rathsman, Phys. Rev. D **58**, 116006 (1998) [hep-ph/9801330].

[62] S. J. Brodsky and P. Huet, Phys. Lett. **B417**, 145 (1998), hep-ph/9707543.

[63] L. Okun and I. Yu. Kobzarev, ZhETF, **43** 1904 (1962) (English translation : JETP **16** 1343 (1963)); L. Okun, in proceedings of the International Conference on Elementary Particles, 4th, Heidelberg, Germany (1967). Edited by H. Filthuth. North-Holland, (1968).

[64] X. Ji, hep-ph/9610369.

[65] X. Ji, Phys. Rev. Lett. **78**, 610 (1997), hep-ph/9603249.

[66] X. Ji, Phys. Rev. **D55**, 7114 (1997), hep-ph/9609381.

[67] O. V. Teryaev, hep-ph/9904376.

[68] A. Harindranath and R. Kundu, Phys. Rev. **D59**, 116013 (1999), hep-ph/9802406.

[69] S. Chang, R. G. Root and T. Yan, Phys. Rev. D **7**, 1133 (1973).

[70] M. Burkardt, Nucl. Phys. **A504**, 762 (1989).

[71] H.-M. Choi and C.-R. Ji, Phys. Rev. **D 58**, 071901 (1998).

[72] K. Hornbostel, S. J. Brodsky and H. C. Pauli, Phys. Rev. D **41**, 3814 (1990).

[73] F. Antonuccio and S. Dalley, Phys. Lett. **B348**, 55 (1995) [hep-th/9411204].

[74] S. J. Brodsky, F. E. Close and J. F. Gunion, Phys. Rev. D **5**, 1384 (1972).

[75] S. J. Brodsky, F. E. Close and J. F. Gunion, Phys. Rev. D **6**, 177 (1972).

[76] S. J. Brodsky, F. E. Close and J. F. Gunion, Phys. Rev. D **8**, 3678 (1973).

[77] M. Diehl, T. Gousset and B. Pire, Phys. Rev. D **62**, 073014 (2000) [hep-ph/0003233].

[78] A. V. Radyushkin, Phys. Lett. **B380**, 417 (1996) [hep-ph/9604317].

[79] X. Ji and J. Osborne, Phys. Rev. D **58**, 094018 (1998) [hep-ph/9801260].

[80] P. A. Guichon and M. Vanderhaeghen, Prog. Part. Nucl. Phys. **41**, 125 (1998) [hep-ph/9806305].

[81] M. Vanderhaeghen, P. A. Guichon and M. Guidal, Phys. Rev. Lett. **80**, 5064 (1998).

[82] A. V. Radyushkin, Phys. Rev. D **59**, 014030 (1999) [hep-ph/9805342].

[83] J. C. Collins and A. Freund, Phys. Rev. D **59**, 074009 (1999) [hep-ph/9801262].

[84] M. Diehl, T. Feldmann, R. Jakob and P. Kroll, Phys. Lett. **B460**, 204 (1999) [hep-ph/9903268].

[85] M. Diehl, T. Feldmann, R. Jakob and P. Kroll, Eur. Phys. J. **C8**, 409 (1999) [hep-ph/9811253].

[86] J. Blumlein and D. Robaschik, Nucl. Phys. **B581**, 449 (2000) [hep-ph/0002071].

[87] M. Penttinen, M. V. Polyakov, A. G. Shuvaev and M. Strikman, Phys. Lett. **B491**, 96 (2000) [hep-ph/0006321].

[88] D. Muller, D. Robaschik, B. Geyer, F. M. Dittes and J. Horejsi, Fortsch. Phys. **42**, 101 (1994) [hep-ph/9812448].

[89] S. J. Brodsky, SLAC-PUB-8649.

[90] G. P. Lepage and S. J. Brodsky, Phys. Lett. **B 87**, 359 (1979).

[91] S. D. Bass, S. J. Brodsky and I. Schmidt, Phys. Rev. D **60**, 034010 (1999) [hep-ph/9901244].

[92] S. J. Brodsky and G. R. Farrar, Phys. Rev. D **11**, 1309 (1975).

[93] G. P. Lepage and S. J. Brodsky, Phys. Rev. Lett. **43**, 545 (1979).

[94] A. Szczepaniak, E. M. Henley and S. J. Brodsky, Phys. Lett. **B243**, 287 (1990).

[95] A. Szczepaniak, Phys. Rev. D **54**, 1167 (1996).

[96] Y. Y. Keum, H. Li and A. I. Sanda, hep-ph/0004173.

[97] H. Li, hep-ph/0012140.

[98] S. J. Brodsky and G. P. Lepage, Phys. Rev. D **24**, 2848 (1981).

[99] S. J. Brodsky, C. Ji, A. Pang and D. G. Robertson, Phys. Rev. D **57**, 245 (1998) [hep-ph/9705221].

[100] S. J. Brodsky and G. P. Lepage, in *C81-04-06.1.4* Phys. Rev. D **24**, 1808 (1981).

[101] E. Braaten and S. Tse, Phys. Rev. D **35**, 2255 (1987).

[102] J. Gronberg *et al.* [CLEO Collaboration], Phys. Rev. **D57**, 33 (1998), hep-ex/9707031; and H. Paar, presented at PHOTON 2000: International Workshop on Structure and Interactions of the Photon Ambleside, Lake District, England, 26-31 Aug 2000.

[103] A. V. Radyushkin, Acta Phys. Polon. **B26**, 2067 (1995) [hep-ph/9511272].

[104] S. Ong, Phys. Rev. D **52**, 3111 (1995).

[105] P. Kroll and M. Raulfs, Phys. Lett. **B387**, 848 (1996) [hep-ph/9605264].

[106] V. L. Chernyak and A. R. Zhitnitsky, Phys. Rept. **112**, 173 (1984).

[107] S. Dalley, hep-ph/0007081.

[108] H. Paar *et al.* CLEO collaboration (to be published); See also J. Boyer *et al.*, *Phys. Rev. Lett.* **56**, 207 (1980); TPC/Two Gamma Collaboration (H. Aihara *et al.*), *Phys. Rev. Lett.* **57**,404 (1986).

[109] G. R. Farrar and H. Zhang, Phys. Rev. Lett. **65**, 1721 (1990).

[110] T. C. Brooks and L. Dixon, Phys. Rev. D **62**, 114021 (2000) [hep-ph/0004143].

[111] N. Isgur and C. H. Llewellyn Smith, Phys. Lett. **B217**, 535 (1989).

[112] A. V. Radyushkin, Phys. Rev. D **58**, 114008 (1998) [hep-ph/9803316].

[113] J. Bolz and P. Kroll, Z. Phys. **A356**, 327 (1996) [hep-ph/9603289].

[114] C. Vogt, hep-ph/0010040.

[115] R. L. Anderson *et al.*, Phys. Rev. Lett. **30**, 627 (1973).

[116] H. M. Sommermann, R. Seki, S. Larson and S. E. Koonin, Phys. Rev. D **45**, 4303 (1992).

[117] S. Brodsky and M. Karliner, in preparation.

[118] S. J. Brodsky, V. S. Fadin, V. T. Kim, L. N. Lipatov and G. B. Pivovarov, JETP Lett. **70**, 155 (1999) [hep-ph/9901229].

[119] A. Donnachie and P. V. Landshoff, hep-ph/0105088.

[120] S. J. Brodsky and D. S. Hwang, in preparation.

[121] S. Brodsky, P.Hoyer, Markus Diehl, S. Peigne, and W. Schäfer, (in preparation).

[122] L. Frankfurt, G. A. Miller and M. Strikman, hep-ph/0010297.

[123] E. M. Aitala *et al.* [E791 Collaboration], Phys. Rev. Lett. **86**, 4773 (2001) [hep-ex/0010044].

[124] E. M. Aitala *et al.* [E791 Collaboration], Phys. Rev. Lett. **86**, 4768 (2001) [hep-ex/0010043].

[125] V. M. Braun, D. Y. Ivanov, A. Schafer and L. Szymanowski, *Phys. Lett. B* **509**, 43 (2001) [hep-ph/0103275].

[126] V. Chernyak, [hep-ph/0103295].

[127] P. Stoler, Few Body Syst. Suppl. **11**, 124 (1999).

[128] G. A. Miller, nucl-th/9910053.

[129] G. A. Miller, S. J. Brodsky and M. Karliner, Phys. Lett. **B481**, 245 (2000) [hep-ph/0002156].

[130] A. S. Carroll *et al.*, Phys. Rev. Lett. **61**, 1698 (1988).

[131] G. R. Court *et al.*, Phys. Rev. Lett. **57**, 507 (1986).

[132] S. J. Brodsky and G. F. de Teramond, Phys. Rev. Lett. **60**, 1924 (1988).

[133] S. J. Brodsky, C. Peterson and N. Sakai, Phys. Rev. D **23**, 2745 (1981).

[134] C. V. Chang and W. Hou, in B Meson," hep-ph/0101162.

[135] S. J. Brodsky and F. S. Navarra, Phys. Lett. B **411**, 152 (1997) [hep-ph/9704348].

[136] S. J. Brodsky and S. Gardner, hep-ph/0108121.

[137] P. Colangelo, G. Nardulli, N. Paver and Riazuddin, Z. Phys. C **45**, 575 (1990).

[138] C. Isola, M. Ladisa, G. Nardulli, T. N. Pham and P. Santorelli, arXiv:hep-ph/0110411.

[139] C. Isola, M. Ladisa, G. Nardulli, T. N. Pham and P. Santorelli, Phys. Rev. D **64**, 014029 (2001) [arXiv:hep-ph/0101118].

[140] M. Ciuchini, E. Franco, G. Martinelli, M. Pierini and L. Silvestrini, Phys. Lett. B **515**, 33 (2001) [hep-ph/0104126].

[141] S. J. Brodsky and I. A. Schmidt, Phys. Lett. **B234**, 144 (1990).

[142] S. J. Brodsky and M. Karliner, Phys. Rev. Lett. **78**, 4682 (1997) [hep-ph/9704379].

[143] S. J. Brodsky, G. P. Lepage and S. F. Tuan, Phys. Rev. Lett. **59**, 621 (1987).

[144] M. Burkardt and B. Warr, Phys. Rev. D **45**, 958 (1992).

[145] A. I. Signal and A. W. Thomas, Phys. Lett. **B191**, 205 (1987).

[146] S. J. Brodsky and B. Ma, Phys. Lett. **B381**, 317 (1996) [hep-ph/9604393].

[147] S. Dalley and I. R. Klebanov, Phys. Rev. D **47**, 2517 (1993) [hep-th/9209049].

[148] F. Antonuccio and S. Dalley, Phys. Lett. **B376**, 154 (1996) [hep-th/9512106].

[149] F. Antonuccio and S. Dalley, Nucl. Phys. **B461**, 275 (1996) [hep-ph/9506456].

[150] S. Dalley and B. van de Sande, Phys. Rev. D **62**, 014507 (2000) [hep-lat/9911035].

[151] J. R. Hiller and S. J. Brodsky, Phys. Rev. D **59**, 016006 (1999) [hep-ph/9806541].

[152] W. Pauli and F. Villars, Rev. Mod. Phys. 21 (1949) 4334.

[153] S. J. Brodsky, J. R. Hiller and G. McCartor, Phys. Rev. D **58**, 025005 (1998) [hep-th/9802120].

[154] S. J. Brodsky, J. R. Hiller and G. McCartor, Phys. Rev. D **60**, 054506 (1999) [hep-ph/9903388].

[155] C. Lanczos, J. Res. Nat. Bur. Stand. **45**, 255 (1950); J.H. Wilkinson, *The Algebraic Eigenvalue Problem* (Clarendon, Oxford, 1965); B.N. Parlett, *The Symmetric Eigenvalue Problem* (Prentice–Hall, Englewood Cliffs, NJ, 1980); J. Cullum and R.A. Willoughby, J. Comput. Phys. **44**, 329 (1981); *Lanczos Algorithms for Large Symmetric Eigenvalue Computations* (Birkhauser, Boston, 1985), Vol. I and II; G.H. Golub and C.F. van Loan, *Matrix Computations* (Johns Hopkins University Press, Baltimore, 1983).

[156] S. A. Paston, E. V. Prokhvatilov, and V. A. Franke, hep-th/9910114.

[157] S. A. Paston, V. A. Franke, and E. V. Prokhvatilov, Theor. Math. Phys. 120 (1999) 1164, hep-th/0002062.

[158] F. Antonuccio, I. Filippov, P. Haney, O. Lunin, S. Pinsky, U. Trittmann and J. Hiller [SDLCQ Collaboration], hep-th/9910012.

[159] O. Lunin and S. Pinsky, hep-th/9910222.

[160] P. Haney, J. R. Hiller, O. Lunin, S. Pinsky and U. Trittmann, Phys. Rev. D **62**, 075002 (2000) [hep-th/9911243].

[161] G. P. Lepage, S. J. Brodsky, T. Huang and P. B. Mackenzie, CLNS-82/522, published in Banff Summer Inst.1981:0083 (QCD161:B23:1981); S. J. Brodsky, T. Huang and G. P. Lepage,

[162] G. Martinelli and C. T. Sachrajda, Amplitude," Phys. Lett. **B190**, 151 (1987).

[163] D. Daniel, R. Gupta and D. G. Richards, Phys. Rev. D **43**, 3715 (1991).

[164] L. Del Debbio, M. Di Pierro, A. Dougall and C. Sachrajda [UKQCD collaboration], Nucl. Phys. Proc. Suppl. **83**, 235 (2000) [hep-lat/9909147].

[165] W. A. Bardeen and R. B. Pearson, Phys. Rev. D **14**, 547 (1976).

[166] M. Burkardt, Phys. Rev. D **54**, 2913 (1996) [hep-ph/9601289].

[167] V. Y. Petrov, M. V. Polyakov, R. Ruskov, C. Weiss and K. Goeke, Phys. Rev. D **59**, 114018 (1999) [hep-ph/9807229].

[168] D. Diakonov and V. Y. Petrov, hep-ph/0009006.

[169] M. B. Hecht, C. D. Roberts and S. M. Schmidt, nucl-th/0008049.

[170] S. J. Brodsky, M. Burkardt and I. Schmidt, distributions," Nucl. Phys. **B441**, 197 (1995) [hep-ph/9401328].

[171] S. J. Brodsky, P. Hoyer, N. Marchal, S. Peigne and F. Sannino, hep-ph/0104291.

[172] V. N. Gribov, Sov. Phys. JETP **29**, 483 (1969) [Zh. Eksp. Teor. Fiz. **56**, 892 (1969)].

[173] S. J. Brodsky and J. Pumplin, Phys. Rev. **182**, 1794 (1969).

[174] S. J. Brodsky and H. J. Lu, Phys. Rev. Lett. **64**, 1342 (1990).

[175] G. Piller and W. Weise, Phys. Rept. **330**, 1 (2000) [hep-ph/9908230].

[176] Y. V. Kovchegov, Phys. Rev. D **55**, 5445 (1997) [hep-ph/9701229].

[177] G. Leibbrandt, Rev. Mod. Phys. **59**, 1067 (1987).

[178] P. V. Landshoff, J. C. Polkinghorne and R. D. Short, Nucl. Phys. B **28**, 225 (1971).

[179] S. J. Brodsky and H. J. Lu, Phys. Rev. D **51**, 3652 (1995) [arXiv:hep-ph/9405218].